Full-Length Articles

Clinical heterogeneity of FTDP-17 caused by *MAPT* N279K mutation in relation to tau PET features

Aya Ikeda MD[1], Hitoshi Shimada MD, PhD[2], Kenya Nishioka MD, PhD[1], Masashi Takanashi MD, PhD[1], Arisa Hayashida MD[1], Yuanzhe Li MD, PhD[1], Hiroyo Yoshino PhD[3], Manabu Funayama PhD[1,3], Yuji Ueno MD, PhD[1], Taku Hatano MD, PhD[1], Naruhiko Sahara PhD[2], Tetsuya Suhara MD, PhD[2], Makoto Higuchi MD, PhD[2], Nobutaka Hattori MD, PhD[1,3]

Affiliations

[1]Department of Neurology, Juntendo University School of Medicine

[2]Department of Functional Brain Imaging Research, National Institute of Radiological Sciences, National Institutes for Quantum and Radiological Science and Technology.

[3]Research Institute for Diseases of Old Age, Graduate School of Medicine, Juntendo University

Supplementary data:

Supplementary case presentation

Supplementary detailed materials and methods

Supplementary Table 1

Supplementary Figure 1

Corresponding authors:

1) Makoto Higuchi, MD, PhD

Department of Functional Brain Imaging Research, National Institute of Radiological Sciences, National Institutes for Quantum and Radiological Science and Technology, 4-9-1 Anagawa, Inage-ku, Chiba 263-8555, Japan.

Phone: +81-43-206-4700; Fax: +81-43-253-0396;

E-mail: higuchi.makoto@qst.go.jp

2) Nobutaka Hattori, MD, PhD

Department of Neurology, Juntendo University, School of Medicine, 2-1-1 Hongo, Bunkyo-ku, Tokyo 113-8421, Japan.

Phone: +81-3-3813-3111; Fax: +81-3-5800-0547;

E-mail: nhattori@juntendo.ac.jp

Disclosure: HS, MH and TS hold a patent on compounds related to the present report (JP 5422782/EP 12 884 742.3), and National Institutes for Quantum and Radiological Science and Technology made a license agreement with APRINOIA Therapeutics Inc. regarding this patent.

Word count for manuscript: 4,152 words

Word count for abstract: 244 words

Character count for title: 81 characters excluding spaces, 95 characters including spaces

Number of references: 51, tables: 2, figures: 3

Keywords: Frontotemporal dementia, MAPT, N279K mutation, tau PET

Author contributions:

Aya Ikeda: acquisition and analysis of data, and drafting the manuscript and figures

Hitoshi Shimada: design of the study, acquisition and analysis of data, and drafting the manuscript and figures

Kenya Nishioka: conception and design of the study, acquisition and analysis of data, and drafting the manuscript and figures

Masashi Takanashi: acquisition and analysis of data, and drafting the manuscript and figures

Arisa Hayashida: acquisition of data

Yuanzhe Li: acquisition of data

Hiroyo Yoshino: acquisition of data

Manabu Funayama: acquisition of data

Yuji Ueno: acquisition of data

Taku Hatano: acquisition of data

Naruhiko Sahara: acquisition of data

Makoto Higuchi: acquisition and analysis of data, and drafting the manuscript

Tetsuya Suhara: critical revision, and drafting the manuscript

Nobutaka Hattori: critical revision, and drafting the manuscript

Financial disclosure

This work was partly supported by Grant-in-Aid for Scientific Research (C) (16K09678) to KN and the young scientists (A) (26713031) to HS from the MEXT/JSPS, Research and

Development Grants for Dementia (16768966) to MH and NH and Practical Research Project for Rare / Intractable Diseases (15ek0109029s0202) to NH from the Japan Agency for Medical Research and Development (AMED).

Abstract

Objectives: The present study aimed to comparatively analyze clinical profiles, tau accumulations, and their correlations in three kindreds afflicted with frontotemporal dementia and parkinsonism linked to chromosome 17 (FTDP-17) due to the *MAPT* N279K mutation.

Methods: Clinical manifestations were analyzed in ten patients with N279K mutant FTDP-17-*MAPT*, who were offspring of the three kindreds. Four participants from these three kindreds underwent PET with [^{11}C]PBB3 to estimate regional tau loads. PET data were compared with postmortem neuropathological findings in two other patients with these pedigrees.

Results: Haplotype assays revealed that these kindreds originated from a single founder. Despite homogeneity of the disease-causing *MAPT* allele, clinical progression was more rapid in two kindreds than in the other, leading to shorter survival after disease onset. PBB3-PET demonstrated that kindreds with slow progression showed mild tau depositions mostly confined to the midbrain and medial temporal areas including the hippocampus and amygdala. In contrast, kindreds with rapid progression showed profoundly increased [^{11}C]PBB3 binding in widespread brain regions in addition to the midbrain and medial temporal regions from an early disease stage. Neuropathological assays also demonstrated characteristic tau pathologies similar to the PET results.

Conclusions: Current tau PET imaging is capable of capturing pathologies constituted of four-repeat tau isoforms characteristic of N279K mutant FTDP-17-*MAPT*, which emerge in the midbrain and medial temporal regions. Our findings also support the view that, in addition to the mutated *MAPT* allele, genetic and/or epigenetic modifiers of tau pathologies lead to heterogeneous clinicopathological features.

Glossary:

AD = Alzheimer's disease; FTLD = frontotemporal lobar degeneration; PSP = progressive supranuclear palsy; CBD = corticobasal degeneration; MAPT = microtubule-associated protein tau; FTD = frontotemporal dementia; PBB3 = pyridinyl-butadienyl-benzothiazole 3; PET = positron emission tomography; PPND = pallidopontonigral degeneration; VOIs = volumes of interest;

Introduction

Tau protein fibrillation has been implicated in Alzheimer's disease (AD), frontotemporal lobar degeneration (FTLD) subtypes and related disorders, which are collectively referred to as tauopathies.[1, 2] FTLD tauopathies, including progressive supranuclear palsy (PSP) and corticobasal degeneration (CBD), are characterized by the deposition of four-repeat tau isoforms in neurons, astrocytes, and oligodendrocytes.[3, 4] Distinct tau isoforms cause ultrastructural and conformational diversity of the pathological fibrils, represented by paired helical filaments in AD and straight filaments in PSP and CBD.[5]

Despite the association between tau conformers, localization of tau lesions, and clinical phenotypes, the symptomatic manifestations and progression of a single tauopathy can vary.[6-9] The *microtubule-associated protein tau* (*MAPT*) haplotypes may account for the clinicopathological characteristics of PSP[10] and frontotemporal dementia (FTD).[6, 11] Moreover, a number of *MAPT* mutations cause familial tauopathies, which are termed frontotemporal dementia and parkinsonism linked to chromosome 17 *MAPT* (FTDP-17-*MAPT*). However, the symptomatic profiles of patients carrying identical *MAPT* mutations are also variable.[12-16]

Evaluation of the correlation between the clinical course and chronological sequence

of regional pathological involvement has been enabled by in vivo positron emission tomography (PET) of tau lesions in humans. The radioligand [^{11}C]pyridinyl-butadienyl-benzothiazole 3 ([^{11}C]PBB3) binds to a wide range of tau fibrils including AD, PSP, and putative CBD tau deposits,[17-19] Other tracers, such as [^{18}F]AV-1451, produce a higher contrast for AD-type tau tangles than it does for four-repeat tau inclusions in PSP and CBD,[20, 21] although [^{18}F]AV-1451 has enabled differentiation between groups of PSP patients and healthy controls.[22] The distinct selectivity of the PET ligands could help identify tau isoforms contributing to unique neurodegenerative pathologies in each individual.[23]

The *MAPT* N279K mutation was originally discovered in the Caucasian pallidopontonegral degeneration (PPND) kindred,[24] and was also found in three Japanese kindreds,[24-26] two of which bore identical mutant *MAPT* allele haplotypes.[27] More recently, our group reported that patients with FTDP-17-*MAPT* in three additional Japanese families with this mutation presented Parkinsonism-dominant clinical phenotypes, similar to the PPND pedigree.[27]

In the present work, we further identified two novel Japanese families with hereditary tauopathy caused by the N279K mutation, and we investigated the abundance and extent of tau deposits in patients harboring the *MAPT* N279K mutation derived from three pedigrees including these two families. As our previous *in vitro* assays demonstrated binding of [^{11}C]PBB3 to N279K mutant four-repeat tau aggregates,[23] [^{11}C]PBB3-PET allowed us to analyze fibrillary tau pathologies in living patients in these families. The haplotypes of all mutant *MAPT* allele-carriers examined here were identical, presumably originating from a single founder. However, there was a profound difference in the progression of functional impairments among these three kindreds, in close association with the severity of PET-detectable tau pathologies.

Methods

Participants and genetic analysis

The current study was approved by the local ethics committees of the Juntendo University School of Medicine and National Institute of Radiological Sciences (NIRS), of which the registration numbers of University hospital medical information network (UMIN) in Japan are #000009863 and #000017978. All participants or caregivers were fully informed and provided written consent. We enrolled patients with suspected FTDP-17 who fulfilled the consensus clinical diagnostic criteria of FTLD[9] and were suspected of having a strong family history of FTD. Four of these participants were derived from a pedigree with the N279K *MAPT* mutation, which was reported previously.[27] We obtained the medical records and neurological findings of the patients, who were examined by at least two neurologists. We also interviewed their family members. DNA analysis was performed as described in the supplementary material and methods.

The N279K *MAPT* mutation was detected in six patients derived from two newly identified kindreds (families A and B), consisting of four males from family A and one male and one female from family B (Table 1 and Figure 1A). The third kindred with the N279K mutation (designated family C in the present study) corresponded to 'family D' in our earlier study.[27] Two previously reported cases of females undergoing autopsy and two new-onset females from this family were analyzed in the present study. All these members of families A, B, and C were born in the same region north of Tokyo. Kaplan-Meier survival estimation and log-rank test were performed using GraphPad Prism®6 (GraphPad Software, Inc., San Diego, CA, USA) to compare the duration of survival after disease onset among these three families.

Tau and amyloid PET imaging

PET scans were performed on four patients with the N279K *MAPT* mutation (A-II-1, B-II-2, C-IV-1 and C-IV-2) at NIRS. Two patients received scans within one year of clinical onset of the disease (at five and twelve months in C-IV-1 and B-II-2), while the other two patients underwent scans relatively late (at three and four years after onset in A-II-1 and C-IV-2, respectively). We also included 13 age- and sex-matched volunteers, who were cognitively intact, as healthy controls (HCs) in the present analysis. They were recruited from the volunteer association at NIRS, and did not have a history of neurological and psychiatric disorders or abnormalities in physical and neurological examinations. PET imaging of tau and amyloid-β lesions with [^{11}C]PBB3 and [^{11}C]Pittsburgh Compound-B ([^{11}C]PiB), respectively, were conducted for these control participants in our previous work.[13] The [^{11}C]PiB-PET data indicated that they were all negative for Aβ deposits.

Radiosynthesis of [^{11}C]PBB3 and [^{11}C]PiB was conducted as described elsewhere.[28, 29] Patients underwent dynamic three-dimensional PET scans, at 50 and 70 min after intravenous injections of [^{11}C]PBB3 (injected dose, 454 ± 79 MBq; molar activity at injection, 104 ± 77 GBq/μmol; chemical purity, 97.1 ± 0.6%) and [^{11}C]PiB (injected dose, 415 ± 75 MBq; molar activity, 70 ± 7 GBq/μmol; chemical purity, 98.8 ± 0.7%), to evaluate tau and Aβ accumulations, respectively. PET data were acquired using a Siemens ECAT EXACT HR+ scanner (CTI PET Systems, Inc., Knoxville, TN), with an axial field of view of 155 mm, providing 63 contiguous 2.46-mm slices with 5.6-mm transaxial and 5.4-mm axial resolutions. Images were then reconstructed using the filtered back-projection algorithm (Hanning filter; cut-off frequency, 0.4 cycle/pixel) to secure methodological consistency with our previous clinical PET works with [^{11}C]PBB3.[17, 18] Attenuation and scatter corrections were applied to these images using the data of a 10-min transmission scan, with a 68Ge-68Ga line source and single-scatter simulation method, respectively.

Three-dimensional T1-weighted magnetic resonance images (repetition time range/echo time range, 7 ms/2.8 ms; field of view [frequency × phase], 260 × 244 mm; matrix dimension, 256 × 256; 170 contiguous axial slices of 1.0 mm thickness) were acquired with a 3-T MRI scanner (Signa HDx; GE Healthcare, WI, USA, or MAGNETOM Verio, Siemens Healthcare, Erlangen, Germany) on the same day as the [^{11}C]PBB3-PET scan.

All images were preprocessed using PMOD software version 3.8 (PMOD Technologies Ltd., Zürich, Switzerland) and Statistical Parametric Mapping software (SPM12, Wellcome Department of Cognitive Neurology, London, UK), operating in the MATLAB software environment (version 9.2; MathWorks, Natick, MA, USA). Data preprocessing and data analysis of the PET images were performed as previously described.[18] Briefly, each PET image was co-registered to individual T1-weighted magnetic resonance images after motion correction, and anatomically normalized into Montreal Neurological Institute standard space (MNI152; Montreal Neurological Institute, Montreal, QC, Canada) using Diffeomorphic Anatomical Registration Through Exponentiated Lie Algebra (DARTEL).[29] We generated parametric images of the standardized uptake value ratio (SUVR) for [^{11}C]PBB3 and [^{11}C]PiB at 30–50 and 50–70 min, respectively, after radioligand injection, using the cerebellar cortex as a reference region. To estimate local tau and Aβ burdens, template volumes of interest (VOIs) were defined in several neocortical and subcortical regions, including gray and white matter of the frontal, parietal, occipital, medial and lateral temporal lobes, and the hippocampus, amygdala, caudate, putamen, globus pallidus, thalamus, anterior and posterior cingulate, substantia nigra (SN), and whole midbrain, using the automated anatomical labeling atlas implemented in PMOD software. They were modified to be devoid of CSF space using CSF maps generated from individual MRI data. Whole gray matter and whole white matter masks were also generated from individual MRI data. In addition to VOI-based quantifications of SUVRs, we

performed a voxel-by-voxel jack-knife examination of parametric SUVR images using SPM12 to statistically assess distributions of areas with an increased [^{11}C]PBB3 retention in each patient compared with 13 HCs.

Neuropathological analysis

The brains of two patients in family C (C-III-3 and C-III-4) were neuropathologically analyzed to examine if the distributions of tau pathologies in these cases agreed with those of other N279K mutant pedigrees, as previously reported.[24, 25, 31, 32] Clinical manifestations of these two patients were reported in our previous work, where C-III-3 and C-III-4 were designated as subjects 6 and 7 from family D, respectively.[27] The pathological analysis methods were described in detail in the supplementary material and methods.

Results

Clinical and genetic analyses

An analysis of *MAPT* haplotypes revealed that all seven patients from families A, B, and C, who were examined here, shared a common single founder (Figure 1A and B). The demography and clinical profiles of all ten patients are summarized in Table 1; detailed clinical information of all patients and family members is described in the supplementary case presentation. Most of the patients manifested motor symptoms as rigid-akinesia parkinsonism at an early clinical stage, followed by exacerbated motor symptoms and cognitive decline within a few years of onset. The efficacy of levodopa treatments was limited. All patients examined were diagnosed with behavioral variant FTD, based on the clinical diagnosis criteria of FTD.[33] Average age at onset was 42.2 ± 5.0 years. Cognitive symptoms were initially characterized by socially inappropriate behavior, apathy,

diminished social interest, and deficits in executive tasks. Apraxia of eyelids and restricted eye movements were less frequent symptoms (42.9%, 4/7). Average age at death was 48.7 ± 6.5 years. Overall disease duration from disease onset to death was very short, averaging 3.6 ± 5.4 years. Despite the haplotypic homogeneity of the mutant *MAPT* allele among the patients, Kaplan-Meier analysis depicted significant differences in the survival proportions between combined A and B families, and family C (p = 0.01 by log-rank test) (Figure 1C). Members of family C had better prognosis than those of families A and B.

PET imaging

Compared with HCs, all scanned patients had larger [^{11}C]PBB3 SUVRs in characteristic brain regions, including neocortical gray and white matter (Table 2 and Figure 2). This was distinct from the gray matter-dominant topology of tau depositions in the AD spectrum,[17, 18] and corresponded to previous [^{11}C]PBB3 autoradiographic findings.[23] Subject C-IV-1 had the shortest interval between onset and PET scans, and exhibited a remarkable increase of [^{11}C]PBB3 SUVRs in the midbrain, including the SN, hippocampus and amygdala, suggesting that tau pathologies could arise from these regions (Figure 2). Tau deposits appeared to expand from the brainstem and limbic areas to the neocortex and subcortical nuclei with disease progression, since subject C-IV-2, who underwent PET assays 4 years after onset, presented more widespread and greater increase of [^{11}C]PBB3 bindinginvolving neocortical white matter, globus pallidus and thalamus than subject C-IV-1 (Table 2).

In line with the notable difference in the rate of progression to death between families A/B and C, a subject from family B (B-II-2), who was scanned 12 months after onset, had even higher levels of [^{11}C]PBB3 retentions in most VOIs than subject C-IV-2, despite the relatively early stage of the clinical course (Figure 2). Radioligand binding in subject A-II-1, a member of family A undergoing PET examinations 3 years after onset, was comparable

with that of subject B-II-2 in the majority of VOIs, although additional increases of [^{11}C]PBB3 SUVRs were noted in several areas, including the parahippocampal gyrus and amygdala (Table 2). Therefore, PET-visible tau pathologies in families A and B seemingly plateaued early during clinical progression. None of the patients were Aβ-positive according to visual and quantitative assessments of [^{11}C]PiB-PET data, which were conducted as in previous studies.[13]

In order to highlight areas with increased [^{11}C]PBB3 retentions on brain maps, we also conducted voxel-based statistical assessments of SUVR images for this tracer. SPM t-maps depicted enhanced [^{11}C]PBB3 radiosignals rather confined to the brainstem and a few other regions including the hippocampus in family C, which was in sharp contrast with increases of radioligand binding in extensive areas containing neocortical gray and white matter in families A and B (Figure 3). This familial difference was observed in subjects with both short and long durations, notwithstanding that areas highlighted in the SPM maps were somewhat increased in a manner dependent on the disease duration.

Neuropathological examinations

We obtained brain tissue from two autopsy cases, subjects C-III-3 and C-III-4, who were members of family C and died 12 and 8 years after disease onset, respectively. The brains of subjects C-III-3 and C-III-4 weighed 930 and 1030 g, respectively (Supplementary Figure 1A, B). Macroscopically, severe atrophic changes were observed in the pallidum and brainstem, while neocortical atrophy was moderate. Furthermore, the SN and locus coeruleus (LC) were depigmented.

Immunohistochemical assays revealed abundant tau lesions, such as neurofibrillary tangles, pretangles, threads, coiled bodies, and tufted astrocytes, in the frontotemporal region, globus pallidus and midbrain, and to a lower extent in other neocortical and limbic

areas and subcortical nuclei. Notably, tau pathology in neocortical white matter primarily consisted of axonal threads, coiled bodies and tufted astrocytes, which were more prominent than those in gray matter (Supplementary Figure 1F, G and Supplementary Table 1). Tau deposits were accompanied by neuronal loss and gliosis, particularly in the basal ganglia and brainstem, including the SN and LC (Supplementary Figure 1C-E and Supplementary Table 1). These alterations were consistent with previously documented neuropathological features of FTDP-17-*MAPT* in Caucasean[31, 32] and Japanese[24, 25] patients with the N279K mutation. Moreover, there was high concordance between pathological characteristics of the two cases, and neurodegenerative pathologies were not overtly related to alpha-synuclein, Aβ, and TDP-43 in the patients' brains.

Discussion

We documented three Japanese families with the N279K FTDP-17-*MAPT* mutation originating from a single founder according to a haplotype analysis. Two of these kindreds (A and B) are newly identified and are characterized by markedly rapid clinical progression, leading to death within 5 years of disease onset. The third kindred (family C) examined here included two previously reported[27] and two novel patients. The rates of clinical advancement were comparable with those of other affected members of this family[27] and carriers of this mutation in different Japanese[24-26] and Caucasian pedigrees,[31, 32, 34, 35] with an approximate post-onset survival period of 10 years. Hence, the present data illustrated a pronounced inter-familial difference in the aggressiveness of the illness, despite the similarity of their mutant *MAPT* allele.

Previous studies reported that patients with FTDP-17-*MAPT*, which could be linked to the same single mutation, demonstrated inter- and intra-familial heterogeneity in clinicopathological features.[12, 13, 16, 36] FTD due to the *MAPT* intron 10 + 16 mutation

presented considerable variation in age at onset and duration of the disease, both between and within families.[12] Furthermore, age at death, disease duration, clinical symptoms, brain atrophy and pathological findings, including tau deposits, were diverse, even among relatives with FTDP-17-*MAPT* caused by the P301L mutation.[16] Taken together with the present results, these observations support the view that the *MAPT* mutation alone may not fully define the clinical and neuropathological outcomes, which could in fact be modulated by other genetic and/or environmental components.

The PET results of the present study provide the first demonstration of heterogeneous neuroimaging phenotypes among patients with FTDP-17-*MAPT* who possess the same pathogenic mutation and *MAPT* allele haplotype. In close association with clinical progress, affected cases in families A and B exhibited extensive increases of [^{11}C]PBB3 binding in neocortical and subcortical areas from an early period after onset. Enhancement of [^{11}C]PBB3 binding, however, was less prominent in patients from family C, who had a longer clinical duration than those from the other two families. These findings indicated that the formation of tau lesions in families A and B occurred rapidly at the peri-onset stage, and then almost plateaued at an early post-onset stage. This was then followed by a prompt evolution of functional deteriorations, resulting in a short lifespan of the affected members after onset. This may also suggest the significance of tau PET as a predictor of the following neurodegenerative processes, resembling findings in patients with AD, who show a tight correlation between baseline retention of a tau PET probe and subsequent longitudinal atrophy of the cortex.[37] Such a notion will be further examined in additional cases with the N279K mutation, and will be expandable to other diverse tauopathies by obtaining time-course evidence from a larger sample size.

The symptomatic profiles of the current N279K mutant cohort were all PSP-like, consistent with the fact that this mutation is commonly related to a

Parkinsonism-predominant phenotypic presentation rather than other tau mutations.[34] However, the manifestations of the two patients from family A were initiated with personality changes (Table 1), raising the possibility of the existence of a variable chronology of neuropsychiatric phenotypes within pedigrees of a common origin. Similar diversities were also noted in members of PPND and Italian families with the N279K mutation,[35] and were conceived to stem from the H1/H2 haplotypes of *MAPT*.[38] Since the Japanese population does not possess the H2 haplotype,[39, 40] the personality-related presentation of initial symptoms observed in family A, but not in the other two families, could be attributed to additional genotypic variations located on the non-mutant *MAPT* allele and/or non-*MAPT* elements.

Parkinsonian symptoms in affected individuals from family C from an early clinical stage are typical of the N279K mutation,[34] and could be induced by involvement of the extrapyramidal tract in tau pathologies. Indeed, a profound increase of [^{11}C]PBB3 binding in subject C-IV-1 with a short post-onset duration was particularly evident in the SN (Table 2), which might be an initiation site of tau fibrillogenesis at a preclinical stage. This may be in line with our previous PET findings, where the nigrostriatal dopaminergic system was disrupted in presymptomatic carriers of the N279K mutation derived from the PPND pedigree.[39] Meanwhile, the origin of tau depositions in members of family A with initial manifestations dominated by psychiatric signs has yet to be clarified. The tau PET data of subject C-IV-1 (in the current study) also suggest that tau pathologies in the amygdala and hippocampal formation emerge early during the clinical course. This might elicit local neuronal death and atrophic changes, as illustrated by an MRI analysis of the above-mentioned N279K mutant carriers at a prodromal disease stage.[39] Although no cognitive impairments were noted in subject C-IV-1, subclinical declines of memory functions related to hippocampal pathologies may occur, and they would be detected by

specific neuropsychological test batteries.

Similar to the advancement of Braak stages of tau pathologies in the AD spectrum,[40] the extent of tau pathologies may reflect the disease progression in N279K mutant cases. However, the tau pathogenesis, even in family C, appeared to be rapidly progressive relative to AD. Moreover, regions and voxels with increased [^{11}C]PBB3 binding in neocortical white matter of mutation carriers from all three families expanded over time, which differed from the gray matter-predominant distribution of tau fibrils in AD. Deposition of tau assemblies in white matter may be a neuropathological characteristic of familial[31, 32, 41, 42] and sporadic[43, 44] FTLDs with an excess of insoluble four-repeat tau isoforms. In mouse models, propagation of four-repeat tau pathologies was provoked by intracranial inoculation of four-repeat tau fibrils,[45] and tau aggregates extracted from the PSP and CBD brains have been found to induce dissemination of tau fibrillogenesis in astrocytes and oligodendrocytes unlike AD brain extracts.[46] Further, the N279K mutant tau may show high propensity to intra-axonal and intercellular propagations to neighboring neurons and glial cells, in light of previous cell-based and neuropathological assays.[47] This property of N279K mutant four-repeat tau isoforms could explain the heavy tau load in white matter and relatively rapid regional expansion of tau accumulations in affected cases. In addition, there should be an additional molecular modifier of tau dissemination, underlying the heterogeneities of tau extent in PET imaging and phenotypic aggressiveness among the three families. Despite these presumptions, there has been no in vivo evidence for cell-to-cell propagations of tau depositions via neural networks in *MAPT* N279K mutant cases, and supportive demonstrations would need to be acquired by longitudinal PET scans of these individuals for tracking temporal changes in the topology of tau depositions.

In family C, the localization of fibrillary tau inclusions in the brains of two autopsied patients corresponded to the spatial extent of tau deposits in previous reports on N279K

mutant cases.[24, 25, 31, 32] On the basis of a neuropathological assay of local tau accumulation seemingly aligned with onsite neuronal loss, the neurotoxicity of overflowing tau species was indicated. Although more intense PET signals in multiple brain areas were observed in patients from families A and B, the regional involvement in these cases was still in general agreement with postmortem findings of the two members of family C and previous neuropathological observations in N279K mutant cases.[48] Therefore, rather than being topological variations, the tau pathologies in families A and B are likely to follow a common trajectory of the tau pathogenesis triggered by the N279K mutation, notwithstanding the rapidness of tau expansions in these kindreds.

A few technical issues need to be considered in the interpretation of the current PET data. A few brain areas, such as the occipital cortex, had high [^{11}C]PBB3 retention *in vivo* despite relatively mild AT8(+) tau accumulations in neuropathological assays (Table 2). This discrepancy could arise from spillover of radioactivity from the superior sagittal sinus leading to overestimation of SUVR values in the occipital VOI. However, no conclusive view on this issue could be constructed at present, as PET and postmortem data were collected from different members of family C, and an analysis of correlations between in vivo imaging and neuropathological assays in the same individuals with N279K and other MAPT mutations will be required for precise evaluations of the binding specificity of [^{11}C]PBB3 for tau pathologies in FTDP-17. Moreover, in vivo off-target binding and non-specific retention of [^{11}C]PBB3 remain undetermined. Our recent in vitro binding assays using human brain homogenates has indicated that [^{11}C]PBB3 does not cross-react with monoamine oxidases A and B,[49] which is in clear distinction from properties of other tau radioligands, including [^{18}F]AV-1451[50] and [^{18}F]THK5351.[51] This observation, however, does not fully ensure the selectivity of [^{11}C]PBB3 for tau fibrils in PET imaging of living patients with tauopathies.

In conclusion, the current study delineated the neuropathological basis of the clinical phenotypes in living patients with FTDP-17-*MAPT*, underscoring the contribution of factors beyond the disease-causative *MAPT* haplotypes and mutations to prompt the spread of tau and clinical progress. Although these modifiers are still unidentified, there could be common accelerators or decelerators of tau pathologies across a wide range of tauopathies. An expansion of the present approach combining tau PET and genetics to a large FTDP-17-*MAPT* pedigree originating from a single founder would facilitate the revelation of such elements. Moreover, our imaging assay has supported the significance of the baseline extent of tau lesions at an early clinical stage as a predictor of rapid and slow subsequent disease progressions. In the event that future clinical assays demonstrate that this can be translated to other four-repeat tauopathies, tau PET would help to stratify an observational or interventional cohort of participants, based on an expected rate of clinical and pathological advancements.

References

1. Ballatore C, Lee VM, Trojanowski JQ. Tau-mediated neurodegeneration in Alzheimer's disease and related disorders. Nat Rev Neurosci 2007;8(9):663-672.

2. Spillantini MG, Goedert M. Tau pathology and neurodegeneration. Lancet Neurol 2013;12(6):609-622.

3. Katsuse O, Iseki E, Arai T, et al. 4-repeat tauopathy sharing pathological and biochemical features of corticobasal degeneration and progressive supranuclear palsy. Acta Neuropathol 2003;106(3):251-260.

4. Murray ME, Kouri N, Lin WL, Jack CR, Jr., Dickson DW, Vemuri P. Clinicopathologic assessment and imaging of tauopathies in neurodegenerative dementias. Alzheimers Res Ther 2014;6(1):1.

5. Quadros A, Ophelia I, Ghania A. Role of tau in Alzheimer's dementia and other neurodegenerative diseases. J Appl Biomed 2007;5:1-12.

6. Morris HR, Gibb G, Katzenschlager R, et al. Pathological, clinical and genetic heterogeneity in progressive supranuclear palsy. Brain 2002;125(Pt 5):969-975.

7. Wakabayashi K, Takahashi H. Pathological heterogeneity in progressive supranuclear palsy and corticobasal degeneration. Neuropathology 2004;24(1):79-86.

8. Lam B, Masellis M, Freedman M, Stuss DT, Black SE. Clinical, imaging, and pathological heterogeneity of the Alzheimer's disease syndrome. Alzheimers Res Ther 2013;5(1):1.

9. Respondek G, Stamelou M, Kurz C, et al. The phenotypic spectrum of progressive supranuclear palsy: a retrospective multicenter study of 100 definite cases. Mov Disord 2014;29(14):1758-1766.

10. Conrad C, Andreadis A, Trojanowski JQ, et al. Genetic evidence for the involvement of tau in progressive supranuclear palsy. Ann Neurol 1997;41(2):277-281.

11. Laws SM, Perneczky R, Drzezga A, et al. Association of the tau haplotype H2 with age at onset and functional alterations of glucose utilization in frontotemporal dementia. Am J Psychiatry 2007;164(10):1577-1584.

12. Janssen JC, Warrington EK, Morris HR, et al. Clinical features of frontotemporal dementia due to the intronic tau 10(+16) mutation. Neurology 2002;58(8):1161-1168.

13. Boeve BF, Tremont-Lukats IW, Waclawik AJ, et al. Longitudinal characterization of two siblings with frontotemporal dementia and parkinsonism linked to chromosome 17 associated with the S305N tau mutation. Brain 2005;128(Pt 4):752-772.

14. Doran M, du Plessis DG, Ghadiali EJ, Mann DM, Pickering-Brown S, Larner AJ. Familial early-onset dementia with tau intron 10 + 16 mutation with clinical features similar to those of Alzheimer disease. Arch Neurol 2007;64(10):1535-1539.

15. Larner AJ. Intrafamilial clinical phenotypic heterogeneity with MAPT gene splice site IVS10+16C>T mutation. J Neurol Sci 2009;287(1-2):253-256.

16. Tacik P, Sanchez-Contreras M, DeTure M, et al. Clinicopathologic heterogeneity in frontotemporal dementia and parkinsonism linked to chromosome 17 (FTDP-17) due to microtubule-associated protein tau (MAPT) p.P301L mutation, including a patient with globular glial tauopathy. Neuropathol Appl Neurobiol 2017;43(3):200-214.

17. Maruyama M, Shimada H, Suhara T, et al. Imaging of tau pathology in a tauopathy mouse model and in Alzheimer patients compared to normal controls. Neuron 2013;79(6):1094-1108.

18. Shimada H, Kitamura S, Shinotoh H, et al. Association between Abeta and tau accumulations and their influence on clinical features in aging and Alzheimer's disease spectrum brains: A [11C]PBB3-PET study. Alzheimers Dement (Amst) 2017;6:11-20.

19. Perez-Soriano A, Arena JE, Dinelle K, et al. PBB3 imaging in Parkinsonian disorders: Evidence for binding to tau and other proteins. Mov Disord 2017;32(7):1016-1024.

20. Marquie M, Normandin MD, Vanderburg CR, et al. Validating novel tau positron emission tomography tracer [F-18]-AV-1451 (T807) on postmortem brain tissue. Ann Neurol 2015;78(5):787-800.

21. Marquie M, Normandin MD, Meltzer AC, et al. Pathological correlations of [F-18]-AV-1451 imaging in non-alzheimer tauopathies. Ann Neurol 2017;81(1):117-128.

22. Schonhaut DR, McMillan CT, Spina S, et al. ^{18}F-flortaucipir tau positron emission tomography distinguishes established progressive supranuclear palsy from controls and Parkinson disease: A multicenter study. Ann Neurol 2017;82:622-634.

23. Ono M, Sahara N, Kumata K, et al. Distinct binding of PET ligands PBB3 and AV-1451 to tau fibril strains in neurodegenerative tauopathies. Brain 2017;140(3):764-780.

24. Yasuda M, Kawamata T, Komure O, et al. A mutation in the microtubule-associated protein tau in pallido-nigro-luysian degeneration. Neurology 1999;53(4):864-868.

25. Arima K, Kowalska A, Hasegawa M, et al. Two brothers with frontotemporal dementia and parkinsonism with an N279K mutation of the tau gene. Neurology 2000;54(9):1787-1795.

26. Tsuboi Y, Baker M, Hutton ML, et al. Clinical and genetic studies of families with the tau N279K mutation (FTDP-17). Neurology 2002;59(11):1791-1793.

27. Ogaki K, Li Y, Takanashi M, et al. Analyses of the MAPT, PGRN, and C9orf72 mutations in Japanese patients with FTLD, PSP, and CBS. Parkinsonism Relat Disord 2013;19(1):15-20.

28. Hashimoto H, Kawamura K, Igarashi N, et al. Radiosynthesis, photoisomerization, biodistribution, and metabolite analysis of 11C-PBB3 as a clinically useful PET probe for imaging of tau pathology. J Nucl Med 2014;55(9):1532-1538.

29. Kimura Y, Ichise M, Ito H, et al. PET Quantification of Tau Pathology in Human Brain with 11C-PBB3. J Nucl Med 2015;56(9):1359-1365.

30. Ashburner J. A fast diffeomorphic image registration algorithm. Neuroimage 2007;38(1):95-113.

31. Wszolek ZK, Pfeiffer RF, Bhatt MH, et al. Rapidly progressive autosomal dominant parkinsonism and dementia with pallido-ponto-nigral degeneration. Ann Neurol 1992;32(3):312-320.

32. Delisle MB, Murrell JR, Richardson R, et al. A mutation at codon 279 (N279K) in exon 10 of the Tau gene causes a tauopathy with dementia and supranuclear palsy. Acta Neuropathol 1999;98(1):62-77.

33. Rascovsky K, Hodges JR, Knopman D, et al. Sensitivity of revised diagnostic criteria for the behavioural variant of frontotemporal dementia. Brain 2011;134(Pt 9):2456-2477.

34. Tsuboi Y, Uitti RJ, Delisle MB, et al. Clinical features and disease haplotypes of individuals with the N279K tau gene mutation: a comparison of the pallidopontonigral degeneration kindred and a French family. Arch Neurol 2002;59(6):943-950.

35. Soliveri P, Rossi G, Monza D, et al. A case of dementia parkinsonism resembling progressive supranuclear palsy due to mutation in the tau protein gene. Arch Neurol 2003;60(10):1454-1456.

36. Lin HC, Lin CH, Chen PL, Cheng SJ, Chen PH. Intrafamilial phenotypic heterogeneity in a Taiwanese family with a MAPT p.R5H mutation: a case report and literature review. BMC Neurol 2017;17(1):186.

37. La Joie R, Visani A, Bourakova V, et al. AV1451-PET CORTICAL UPTAKE AND REGIONAL DISTRIBUTION PREDICT LONGITUDINAL ATROPHY IN ALZHEIMER'S DISEASE. Alzheimer's & Dementia: The Journal of the Alzheimer's Association 2017;13(7):P769.

38. Woodruff BK, Baba Y, Hutton ML, et al. Haplotype-phenotype correlations in kindreds with the N279K mutation in the tau gene. Arch Neurol 2004;61(8):1327; author reply 1327.

39. Miyoshi M, Shinotoh H, Wszolek ZK, et al. In vivo detection of neuropathologic changes in presymptomatic MAPT mutation carriers: a PET and MRI study. Parkinsonism Relat Disord 2010;16(6):404-408.

40. Braak H, Braak E. Neuropathological stageing of Alzheimer-related changes. Acta Neuropathol 1991;82(4):239-259.

41. Sima AA, Defendini R, Keohane C, et al. The neuropathology of chromosome 17 - linked dementia. Ann Neurol 1996;39(6):734-743.

42. Spillantini MG, Goedert M, Crowther RA, Murrell JR, Farlow MR, Ghetti B. Familial multiple system tauopathy with presenile dementia: a disease with abundant neuronal and glial tau filaments. Proc Nat Acad Sci U S A 1997;94(8):4113-4118.

43. Forman MS, Zhukareva V, Bergeron C, et al. Signature tau neuropathology in gray and white matter of corticobasal degeneration. Am J Pathol 2002;160(6):2045-2053.

44. Williams DR, Holton JL, Strand C, et al. Pathological tau burden and distribution distinguishes progressive supranuclear palsy-parkinsonism from Richardson's syndrome. Brain 2007;130(6):1566-1576.

45. Clavaguera F, Bolmont T, Crowther RA, et al. Transmission and spreading of tauopathy in transgenic mouse brain. Nat Cell Biol 2009;11:909-913.

46. Narasimhan S, Guo JL, Changolkar L, et al. Pathological Tau Strains from Human Brains Recapitulate the Diversity of Tauopathies in Nontransgenic Mouse Brain. J Neurosci 2017;37:11406-11423.

47. Wren MC, Zhao J, Liu CC, et al. Frontotemporal dementia-associated N279K tau mutant disrupts subcellular vesicle trafficking and induces cellular stress in iPSC-derived neural stem cells. Mol Neurodegener 2015;10:46.

48. Slowinski J, Dominik J, Uitti RJ, Ahmed Z, Dickson DD, Wszolek ZK. Frontotemporal dementia and Parkinsonism linked to chromosome 17 with the N279K tau mutation. Neuropathology 2007;27(1):73-80.

49. Ni R, Ji B, Ono M, et al. Comparative In Vitro and In Vivo Quantifications of Pathologic Tau Deposits and Their Association with Neurodegeneration in Tauopathy Mouse Models. J Nucl Med 2018;59:960-966.

50. Vermeiren C, Motte P, Viot D, et al. The tau positron-emission tomography tracer AV-1451 binds with similar affinities to tau fibrils and monoamine oxidases. Mov Disord 2018;33:273-281.

51. Ng KP, Pascoal TA, Mathotaarachchi S, et al. Monoamine oxidase B inhibitor,

selegiline, reduces ^{18}F-THK5351 uptake in the human brain. Alzheimers Res Ther 2017;9:25.

Figure legends

Figure 1. Genetic and clinical profiles of FTDP-17-*MAPT* patients derived from three families with the N279K *MAPT* mutation

(A) Pedigrees of families A, B and C. Each family originated from the same rural area with autosomal dominant inheritance, manifesting young-onset Parkinsonism and progressive cognitive decline. Filled symbols denote patients with Parkinsonism and cognitive decline, while 'm' indicates confirmed carriers of the N279K mutation. Slashed symbols denote deceased individuals; autopsied cases are indicated by asterisks. (B) Haplotype analysis of the patients showed similar gene dosage as measured by GeneMapper and identical single nucleotide polymorphisms (SNPs) in the region of *MAPT*, indicating that all these families share a common founder. (C) Kaplan-Meier survival curves for 10 patients from combined A and B families (dashed line; n = 6) and family C (solid line; n = 4). Log-rank test indicated that families A and B exhibited shorter post-onset lifespan than family C (p = 0.01).

Figure 2. [^{11}C]PBB3-PET images of representative cognitively healthy control and patients with N279K mutant FTDP-17-*MAPT*

Axial parametric SUVR images, acquired at 30–50 min after radioligand injection, were superimposed on the corresponding magnetic resonance images. All patients showed noticeable uptake of [^{11}C]PBB3 in multiple brain regions and the superior sagittal sinus (yellow arrowheads).

Figure 3. Localization of increased [^{11}C]PBB3 retention in each patient compared with HCs

Voxels with an increase of [^{11}C]PBB3 SUVR was highlighted in coronal (top), axial (middle) and sagittal (bottom) SPM t-maps. A patient with the shortest disease duration (C-IV-1) already showed remarkable enhancement of [^{11}C]PBB3 binding in several areas including the midbrain (white arrows) and medial temporal cortex (yellow arrowheads). Members of families A and B exhibited more extensive [^{11}C]PBB3 radiosignals particularly in neocortical gray and white matter than cases derived from family C.

Figure 1

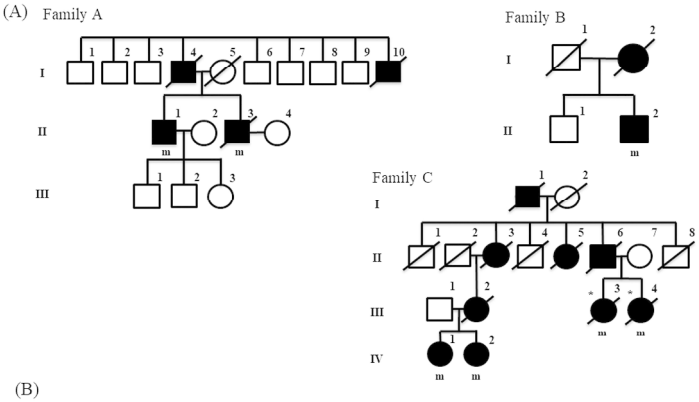

(B)

		Family A				Family B				Family C					
		A-II-1		A-II-3		B-II-2		C-III-3		C-III-4		C-IV-1		C-IV-2	
	D17S805	231	221	231	221	231	231	231	231	231	219	231	219	231	219
	D17S798	231	231	231	231	231	231	231	231	231	229	231	229	231	229
	D17S800	247	247	247	247	249	241	247	245	247	241	247	241	247	241
	D17S810	241	241	241	241	241	241	241	241	241	241	241	241	241	241
	rs1467967	A	A	A	G	A	A	A	G	A	A	A	G	A	G
	rs242557	G	G	G	G	G	G	G	A	G	A	G	A	G	A
	rs3785883	G	G	G	G	G	G	G	G	G	G	G	A	G	A
MAPT	rs2471738	T	C	T	T	T	T	T	C	T	T	T	C	T	C
	c.837T>G	G	T	G	T	G	T	G	T	G	T	G	T	G	T
	del-in9	no	no	no	no	no	no	no	no	no	no	no	no	no	no
	rs7521	G	A	G	G	G	G	G	A	G	G	G	G	G	G
	D17S806	183	151	183	151	175	175	183	187	175	173	183	155	183	155
	D17S797	172	172	172	172	172	172	172	170	172	172	172	172	172	172
	D17S809	270	268	270	276	270	278	270	278	270	270	270	276	270	276

(C)

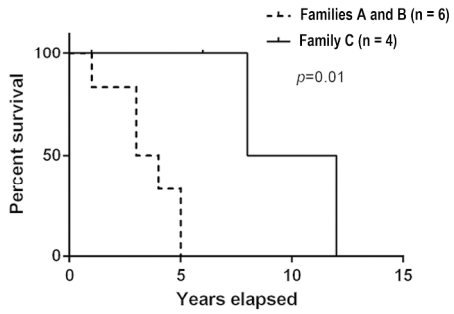

Figure 1 (high-resolution image is provided at the end of the supplement for review)

266x441mm (300 x 300 DPI)

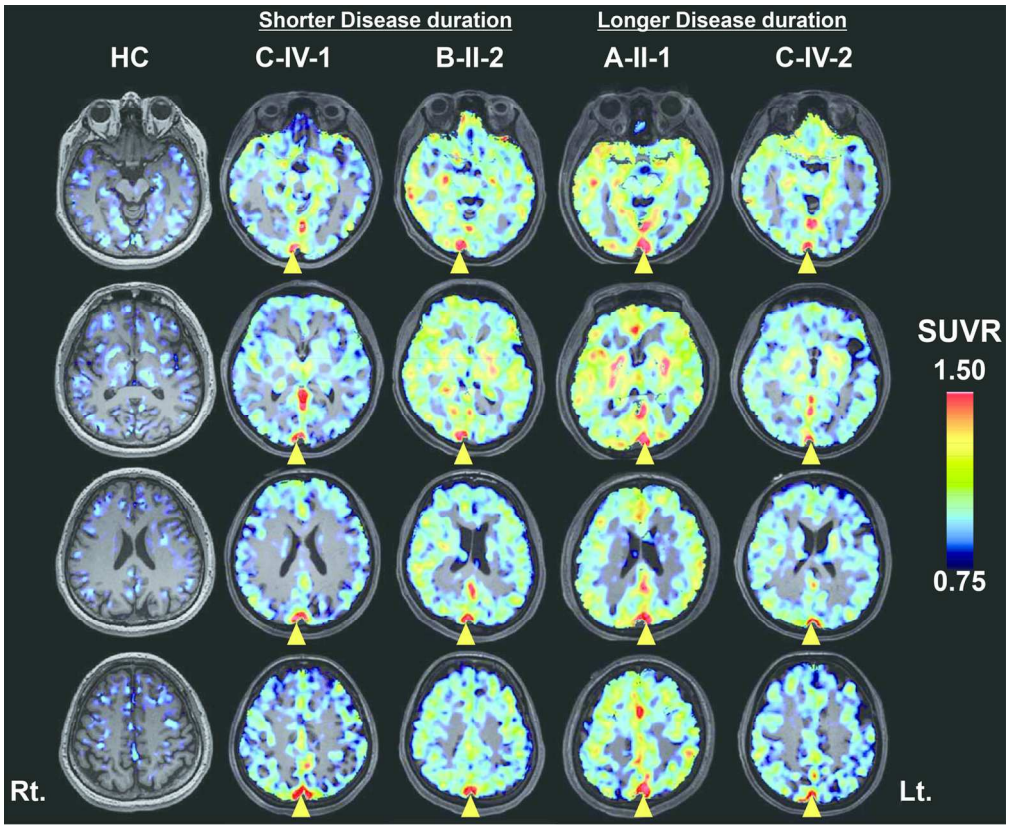

Figure 2 (high-resolution image is provided at the end of the supplement for review)

139x113mm (300 x 300 DPI)

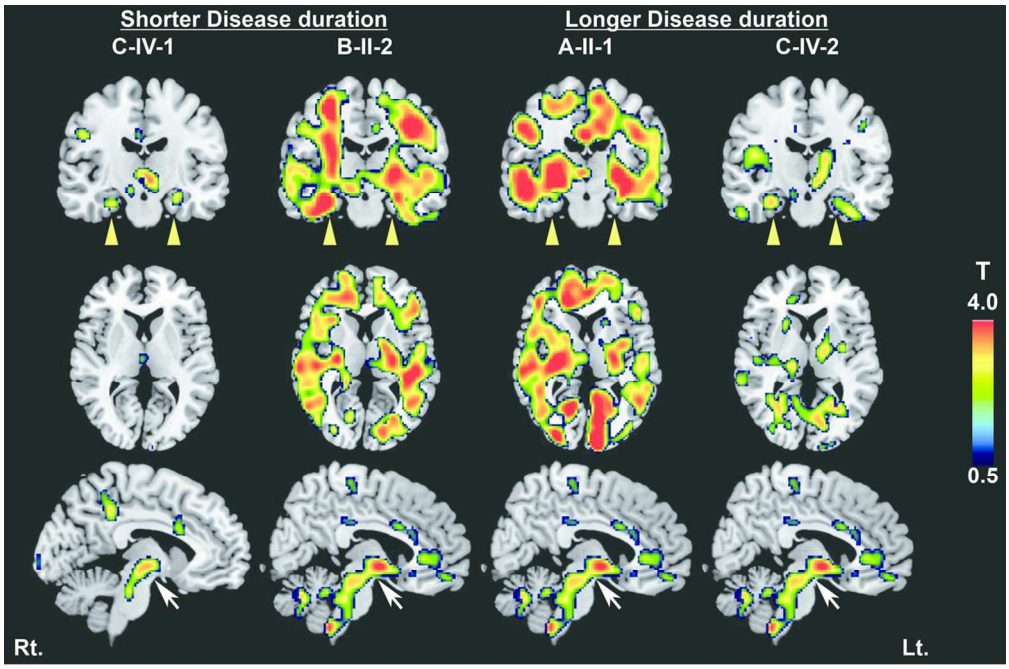

Figure 3 (high-resolution image is provided at the end of the supplement for review)

111x73mm (300 x 300 DPI)

Table 1. Demography and clinical characteristics of affected members of families A, B, and C.

	A-I-4	A-I-10	A-II-1*	A-II-3	B-I-2	B-II-2*	C-III-3†	C-III-4†	C-IV-1	C-IV-2*	
Gender	Male	Male	Male	Male	Female	Male	Female	Female	Female	Female	Male 5 (50%)
Age at disease onset (yrs)	50	40	41	38	50	40	42	43	44	34	42.2 ± 4.96
Age at death (yrs)	55	41	NA	41	55	44	54	51	NA	NA	48.7 ± 6.50
Age at examination (yrs)	NA	NA	44	39	NA	41	NA	NA	44	40	41.6 ± 2.30
Disease duration at examination (yrs)	5	NA	3	1	5	1	NA	NA	0.5	6	3.07 ± 2.28
Initial symptom at onset	Gait disturbance	Character changes	Parkinsonism	Character changes	Parkinsonism	Parkinsonism	Parkinsonism	Parkinsonism	Parkinsonism	Parkinsonism	
Type of disorder	NA	NA	bvFTD	bvFTD	NA	bvFTD	PSP	PSP	NA	bvFTD	
Character changes	NA	+	+	+	NA	+	+	+	+	+	100% (8/8)
MMSE (/30)	NA	NA	NA	NA	NA	23	NA	NA	30	29	
FAB (/18)	NA	NA	NA	NA	NA	16	NA	NA	15	16	
Parkinsonism	+	+	+	+	+	+	+	+	+	+	100% (10/10)
Akinesia	NA	NA	+	+	NA	+	+	+	+	+	100% (7/7)
Rigidity	NA	NA	+	+	NA	+	+	+	+	+	100% (7/7)
Tremor	NA	NA	+	+	NA	+	-	-	-	+	57.1% (4/7)
Response for levodopa	NA	NA	-	-	NA	-	-	-	-	-	0% (0/7)
Apraxia of eyelid	NA	NA	+	-	NA	-	+	+	-	-	42.9% (3/7)
Abnormal eye movements	NA	NA	+	-	NA	-	+	+	-	-	42.9% (3/7)
Prognosis	worsened	worsened	worsened	worsened	worsened	worsened	worsened	worsened	NA	mild	
SBR of DAT scan (right/left)			0.92/0.87			1.29/0.15			1.32/0.07	2.57/0.55	

Cases included tau PET study are highlighted in light grey. Abbreviations: *, proband; †; autopsy case; MMSE, mini-mental state examination; FAB, frontal assessment battery; NA, not applicable/not available; DAT, dopamine transporter; SBR, specific binding ratio; bvFTD, behavior variant frontotemporall dementia; PSP, progressive supranuclear palsy.

Table 2. [^{11}C]PBB3-PET data in subjects A-II-1, B-II-2, C-IV-1, and C-IV-2 in comparison with HCs.

	Patients with N279K mutant FTDP-17-*MAPT*				HCs
	C-IV-1	B-II-2	A-II-1	C-IV-2	
Estimated duration between 1 to 5 in mRS (yrs)	NA	4	5	7	
Speed of disease progression	NA	Rapid	Rapid	Slow	
UPDRS motor subscale total score	9	3	39	6	0 (0)
MMSE	25	22	NA	29	29.1 (1.1)
Disease duration (yrs)	Shorter		Longer		
	0.6	1	3	4	
	[^{11}C]PBB3 SUVR				
Frontal lobe, GM	0.91	1.01	1.04	0.91	0.86 (0.05)
WM	0.84	1.01	1.04	0.91	0.83 (0.04)
Parietal lobe, GM	0.83	0.98	1.05	0.91	0.80 (0.06)
WM	0.80	0.99	1.03	0.90	0.78 (0.05)
Lateral Temporal lobe, GM	0.95	1.08	1.11	1.02	0.89 (0.05)
WM	0.87	1.05	1.06	0.97	0.85 (0.04)
Medial Temporal lobe, GM	1.03	1.08	1.12	1.09	0.92 (0.06)
WM	0.92	1.10	1.08	1.00	0.87 (0.05)
Occipital lobe, GM	0.96	1.04	1.11	0.99	0.84 (0.05)
WM	0.90	1.03	1.08	0.97	0.83 (0.04)
Hippocampus	1.00	1.10	1.06	1.02	0.89 (0.05)
Amygdala	1.02	0.97	1.13	1.03	0.88 (0.05)
Caudate	0.83	0.87	0.91	0.91	0.82 (0.05)
Putamen	0.95	1.17	1.24	1.08	0.97 (0.06)
Pallidum	0.98	1.23	1.36	1.13	0.97 (0.07)
Thalamus	0.96	1.10	1.07	1.08	0.90 (0.07)
Anterior cingulate	0.91	1.00	1.13	0.93	0.86 (0.04)
Posterior cingulate	0.97	1.04	1.11	1.04	0.89 (0.06)
Substantia nigra	1.04	1.07	1.00	1.01	0.85 (0.05)
Midbrain	0.93	1.01	1.01	0.99	0.83 (0.05)
Whole GM	0.95	1.05	1.11	0.97	0.88 (0.05)
Whole WM	0.80	0.96	0.99	0.89	0.85 (0.04)

Abbreviations: HCs, healthy controls; mRS, modified ranking scale; UPDRS, unified Parkinson's disease rating scale; MMSE, mini-mental state examination; GM, gray matter; WM, white matter; SUVR, standardized uptake value ratio; NA, not applicable/not available.

Note: In HCs, each value is presented as mean ± SD. As for the PBB3-SUVR value of each patient, Z-scores ≥ +1SD and < +2SD of HCs are highlighted in blue, scores ≥ +2SD and < +3SD of HCs are highlighted in yellow, and scores ≥ +3SD of HCs are highlighted in red.

Supplementary data

Case presentation

Family A

A-II-1: At the age of 42 years, the patient was frequently falling down, and he noticed a tremor in his right lower limb. He was diagnosed with Parkinson's disease (PD) in another hospital, presenting with rigidity, akinesia, resting tremor, and decreasing of facial expression. His temperament changed, with violent behavior becoming more prominent toward his family. At the age of 44 years, he was admitted to Juntendo University Hospital. He manifested rigid-akinesia Parkinsonism and prominent psychosis of visual hallucination, delusion, and irritability. Cognitive test indices were 29/30 in the Mini-Mental State Examination (MMSE), and 17/18 in the frontal assessment battery (FAB). Brain MRI indicated severe atrophic changes in the temporal lobe and parahippocampal gyrus. [1-3] I-FP-CIT dopamine transporter (DAT) scan, which was conducted using single photon emission computed tomography (SPECT), indicated severe reduction of specific binding ratio (SBR) as follows: right = 0.92, left = 0.87. Three-dimensional stereotactic surface projection (3D-SSP) analysis of brain SPECT showed hypoperfusion in the frontotemporal lobe.

A-I-4: Parkinsonism symptoms appeared in the patient at the age of 54 years, and cognitive decline became exacerbated the following year. At the age of 56 years, the patient had a fall and died of head trauma.

A-I-10: The patient experienced Parkinsonism at the age of 40 years. He died 1 year later.

A-II-3: The patient began to manifest Parkinsonism symptoms at the age of 38 years. He harbored *MAPT* N279K, which was proven by our genetic test. Body weight loss soon became prominent (-20 kg / 2 years). The patient died in the bath 3 years after disease onset.

Family B

B-II-2: The patient noticed akinesia in the right upper and lower limbs at the age of 40 years. He had difficulty swallowing 6 months after disease onset, which is when he attended Juntendo University Hospital. He presented with rigidity on the right side against levodopa treatment and progressive cognitive decline at the initial examination. The indices of cognitive tests were as follows: 16/18 by FAB and 23/30 by MMSE. He also had

prominently complicated motor aphasia, which was categorized as primary progressive aphasia. His mood was always euphoric and calm, without psychosis or violent tendencies. Two years after the first examination, the scores were exacerbated to 9/18 and 20/30 by FAB and MMSE, respectively. His Parkinsonism had also rapidly worsened during the first 2 years. Brain MRI indicated severe atrophic changes in the temporal lobe and parahippocampal gyrus. A DAT scan indicated severe reduction of SBR; right=0, left=0. 3D-SSP analysis of brain SPECT demonstrated hypoperfusion in the frontotemporal lobe, with prominence on the left side. After admission to our hospital, he lived in the faculty. At the age of 44, he was found with cardiopulmonary arrest; the cause of death was unknown.

B-I-2: The patient manifested Parkinsonism from the early fifth decade. She died at age 55. Her cause of death was unknown due to a lack of medical information.

Family C

C-IV-1: The patient noticed akinesia in the right lower limb at the age of 34 years. The year after akinesia, tremor emerged in the right upper limb. Her two aunts (C-III-3 and C-III-4) were pathologically confirmed as having frontotemporal dementia, with proven N279K mutation. Thus, we assessed and confirmed that C-IV-1 was also positive for *MAPT* N279K. Brain MRI indicated mild atrophic changes in the temporal lobe. A DAT scan indicated severe reduction of SBR; right=1.32, left=0. 3D-SSP analysis of brain SPECT showed hypoperfusion in the bilateral frontal lobe. At age 39, her cognitive test indices indicated 12/18 by FAB. At 40 years, her cognitive decline had exacerbated. She always needed help when she walked and she had marked aphasia. She often just whispered and found it difficult to communicate with others. Her modified rating scale changed to 5.

C-IV-2: The patient presented with akinesia in the right upper and lower limbs at Juntendo University Hospital at the age of 44 years. At the first neurological examination, she could communicate with others; she showed no signs of cognitive decline or verbal problems. She showed rigidity and akinesia in her right upper and lower limbs. Her Hoehn and Yahr stage was I. The test indices related to cognitive function were 30/30 by MMSE and 15/18 by FAB. Brain MRI indicated no atrophic changes. DAT scan indicated severe reduction of SBR on the left side; right=2.57, left=0.55. Generally, she showed mild Parkinsonism. She underwent [^{11}C]PBB3 PET

analysis 5 months after disease onset.

C-I-1, C-II-3, C-II-5, C-II-6, and C-III-2 were diagnosed with Parkinson's disease or atypical Parkinsonism during their lifetime. Details of the respective cases are unknown.

Supplementary detailed materials and methods

DNA analysis

Genomic DNA was extracted from peripheral blood using standard protocols. DNA was amplified using direct PCR and then sequenced using the Sanger method, with a BigDye Terminators v1.1 Cycle Sequencing Kit and 3130 Genetic Analyzer (Life Technologies, Foster City, CA, USA). All coding exons and exon-intron boundaries of exons 1 to 10 of *MAPT* were screened. Sequences and PCR conditions have been described in detail in our previous reports.[26]

Haplotype analysis

Haplotype analyses of *MAPT* in seven probands (two cases from family A, one case from family B, and four cases from family C) were performed using seven microsatellite makers (D17S805, D17S798, D17S800, D17S810, D17S806, D17S797 and D17S809), five single nucleotide polymorphisms (SNPs) (rs1467967, rs242557, rs3785883, rs2471738 and rs7521), and an intronic microdeletion (del-in9). Alleles were sized using the GeneMapper (Life Technologies, Carlsbad, CA, USA). A total of 5 SNPs and del-in9 were analyzed using direct Sanger sequencing.

Pathological analysis

The brains were fixed with 15% buffered formalin for 7 days. Multiple tissue blocks of selected anatomical structures were dissected and embedded in paraffin. Tissue blocks were sliced into 6-μm-thick sections, and were used for histochemical staining, including hematoxylin and eosin (HE), Klüver-Barrera (KB) stain, Kleihauer-Betke stain, and Gallyas-Braak (GB) silver impregnation. Immunohistochemistry was also performed for these sections using a monoclonal anti-phosphorylated tau antibody (AT8, Thermo Fisher Scientific, Waltham, MA, USA), anti-phosphorylated alpha-synuclein monoclonal antibody (pSyn#64) (Wako, Osaka, Japan), anti-phosphorylated TDP-43 monoclonal antibody (Ser409/410) (Cosmo bio, Tokyo, Japan), and anti-amyloid β (1-42) monoclonal antibody (IBL, Gunma, Japan). Reacted antibodies were captured using biotinylated secondary antibodies, and visualized using the peroxidase-polymer based method, with a Histofine

Simple Stain MAX-PO kit (Nichirei, Tokyo, Japan) and diaminobenzidine as the chromogen.

Supplementary Table 1. Semiquantitative analysis of neuropathology in two autopsy cases (C-III-3 and C-III-4)

	Neuronal loss	Gliosis	NFTs	Grains	Threads and coiled bodies	Astrocytic inclusions
Frontal cortex	-	+	+	+	++	-
Frontal subcortex		+			+++	-
Temporal cortex	-	-	+	+	+	-
Temporal subcortex		+			++	-
Internal capsule		+++			+	-
Amygdala	-	+	+	+	++	-
Hippocampus	-	++	+	+	++	-
Para hippo	-	+	+	+	+	-
Gyrus cinguli	-	-	+	-	+	-
Putamen	-	+	+	+	++	-
Gp lateral segment	+++	+++	++	++	+++	-
Gp medial segment	+++	+++	++	++	+++	-
Subthalamus	+++	+++				-
Thalamus	++	++	++	+	++	-
Tegmentum mesencephali	++	+++	+++	+++	+++	-
Oculomotor nerve nuclei	++	+++	++	++	+++	-
Substantia nigra	+++	+++	++	++	++	-
Cerebral peduncle		+			+	-
Tegmentum of pons	++	+++	++	++	++	-
Locus coeruleus	-	+	+	+	+	-
Pontine N	-	+	++	++	++	-
Inf Olive	-	+	++	++	++	-
Pillamis		+			+	-
Cerebellar dentate	-	+	+	+	++	-
Cerebellar cort	-	-	-	-	-	-
Lateral collum		+			+	-
Ant horn	-	-	-	-	-	-

(-), absent; (+), occasional; (++), mild; (+++), frequent.

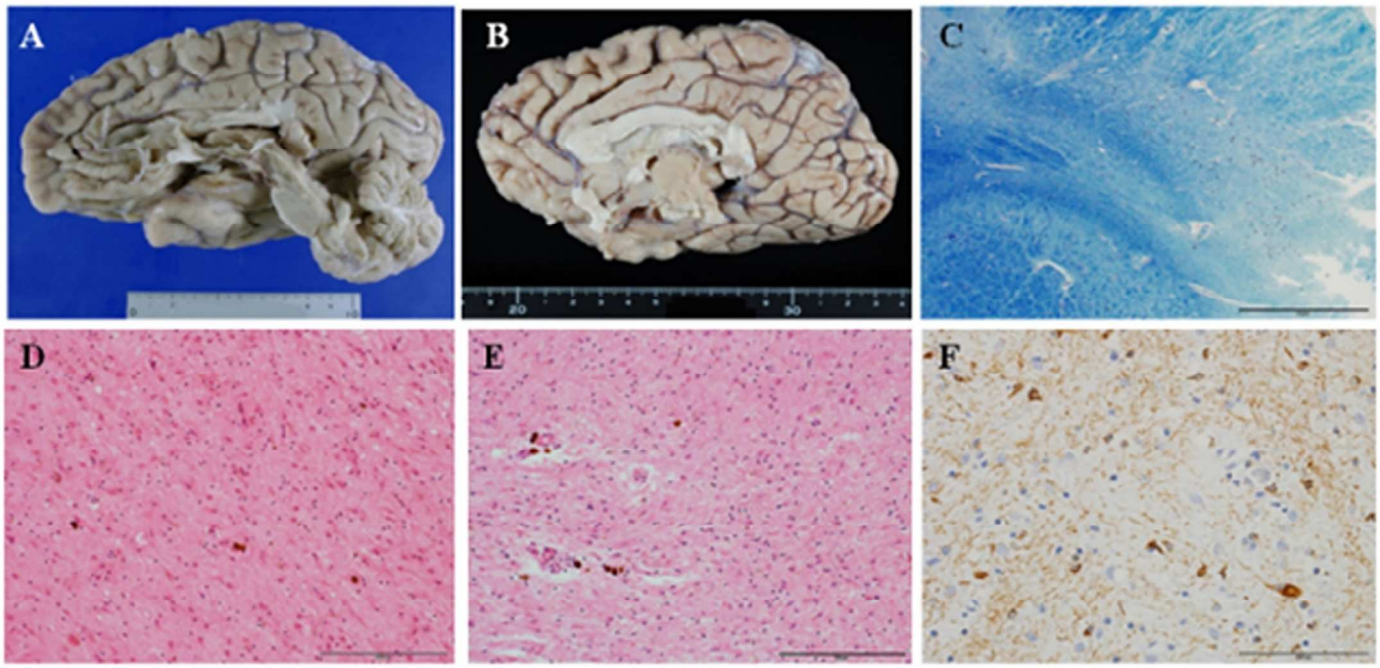

Supplementary Figure 1. Pathological findings in two affected members of family C

(A, B) Macroscopic pictures of the brains of subjects C-III-3 (A) and C-III-4 (B). Both brains showed marked atrophic changes in the frontal lobe and brainstem. (C) Severe loss of pigmented neurons in the substantia nigra (SN; Kleihauer-Betke stain). (D, E) Hematoxylin and eosin (HE) staining also revealed profound neuronal loss and gliosis in the globus pallidus (D) and SN (E). (F) Tau-positive neuronal and glial inclusions, composed of neurofibrillary tangles, threads and coiled bodies in the globus pallidus (AT8 immunostaining). Panels B-F were derived from subject C-III-4.

Full-Length Articles

Clinical heterogeneity of FTDP-17 caused by *MAPT* N279K mutation in relation to tau PET features

Aya Ikeda MD[1], Hitoshi Shimada MD, PhD[2], Kenya Nishioka MD, PhD[1], Masashi Takanashi MD, PhD[1], Arisa Hayashida MD[1], Yuanzhe Li MD, PhD[1], Hiroyo Yoshino PhD[3], Manabu Funayama PhD[1,3], Yuji Ueno MD, PhD[1], Taku Hatano MD, PhD[1], Naruhiko Sahara PhD[2], Tetsuya Suhara MD, PhD[2], Makoto Higuchi MD, PhD[2], Nobutaka Hattori MD, PhD[1,3]

Affiliations

[1]Department of Neurology, Juntendo University School of Medicine

[2]Department of Functional Brain Imaging Research, National Institute of Radiological Sciences, National Institutes for Quantum and Radiological Science and Technology.

[3]Research Institute for Diseases of Old Age, Graduate School of Medicine, Juntendo University

Supplementary data:

Supplementary case presentation

Supplementary detailed materials and methods

Supplementary ~~table~~Table 1

Supplementary Figure 1

Corresponding authors:

1) Makoto Higuchi, MD, PhD

Department of Functional Brain Imaging Research, National Institute of Radiological Sciences, National Institutes for Quantum and Radiological Science and Technology, 4-9-1 Anagawa, Inage-ku, Chiba 263-8555, Japan.

Phone: +81-43-206-4700; Fax: +81-43-253-0396;

E-mail: higuchi.makoto@qst.go.jp

2) Nobutaka Hattori, MD, PhD

Department of Neurology, Juntendo University, School of Medicine, 2-1-1 Hongo, Bunkyo-ku, Tokyo 113-8421, Japan.

Phone: +81-3-3813-3111; Fax: +81-3-5800-0547;

E-mail: nhattori@juntendo.ac.jp

Disclosure: HS, MH and TS hold a patent on compounds related to the present report (JP 5422782/EP 12 884 742.3), and National Institutes for Quantum and Radiological Science and Technology made a license agreement with APRINOIA Therapeutics Inc. regarding this patent.

Word count for manuscript: ~~3,815~~4,152 words

Word count for abstract: ~~243~~244 words

Character count for title: 81 characters excluding spaces, 95 characters including spaces

Number of references: ~~45~~51, tables: 2, figures: 3

Keywords: Frontotemporal dementia, MAPT, N279K mutation, tau PET

Author contributions:

Aya Ikeda: acquisition and analysis of data, and drafting the manuscript and figures

Hitoshi Shimada: design of the study, acquisition and analysis of data, and drafting the manuscript and figures

Kenya Nishioka: conception and design of the study, acquisition and analysis of data, and drafting the manuscript and figures

Masashi Takanashi: acquisition and analysis of data, and drafting the manuscript and figures

Arisa Hayashida: acquisition of data

Yuanzhe Li: acquisition of data

Hiroyo Yoshino: acquisition of data

Manabu Funayama: acquisition of data

Yuji Ueno: acquisition of data

Taku Hatano: acquisition of data

Naruhiko Sahara: acquisition of data

Makoto Higuchi: acquisition and analysis of data, and drafting the manuscript

Tetsuya Suhara: critical revision, and drafting the manuscript

Nobutaka Hattori: critical revision, and drafting the manuscript

Financial disclosure

This work was partly supported by Grant-in-Aid for Scientific Research (C) (16K09678) to KN and the young scientists (A) (26713031) to HS from the MEXT/JSPS, Research and

Development Grants for Dementia (16768966) to MH and NH and Practical Research Project for Rare / Intractable Diseases (15ek0109029s0202) to NH from the Japan Agency for Medical Research and Development (AMED).

Abstract

Objectives: The present study aimed to comparatively analyze clinical profiles, tau accumulations, and their correlations in three kindreds afflicted with frontotemporal dementia and parkinsonism linked to chromosome 17 (FTDP-17) due to the *MAPT* N279K mutation.

Methods: Clinical manifestations were analyzed in ten patients with N279K mutant FTDP-17-*MAPT*, who were offspring of the three kindreds. Four participants from these three kindreds underwent PET with [^{11}C]PBB3 to estimate regional tau loads. PET data were compared with postmortem neuropathological findings in two other patients with these pedigrees.

Results: Haplotype assays revealed that these kindreds originated from a single founder. Despite homogeneity of the disease-causing *MAPT* allele, clinical progression was more rapid in two kindreds than in the other, leading to shorter survival after disease onset. PBB3-PET demonstrated that kindreds with slow progression showed mild tau depositions mostly confined to the midbrain and medial temporal areas including the hippocampus and amygdala. In contrast, kindreds with rapid progression showed ~~profound PET-detectable tau pathologies~~profoundly increased [^{11}C]PBB3 binding in widespread brain regions in addition to the midbrain and medial temporal regions from an early disease stage. Neuropathological assays also demonstrated characteristic tau pathologies similar to the PET results.

Conclusions: Current tau PET imaging is capable of capturing pathologies constituted of four-repeat tau isoforms characteristic of N279K mutant FTDP-17-*MAPT*, which emerge in the midbrain and medial temporal regions. Our findings also support the view that, in addition to the mutated *MAPT* allele, genetic and/or epigenetic modifiers of tau pathologies lead to heterogeneous clinicopathological features.

Glossary:

AD = Alzheimer's disease; FTLD = frontotemporal lobar degeneration; PSP = progressive supranuclear palsy; CBD = corticobasal degeneration; MAPT = microtubule-associated protein tau; FTD = frontotemporal dementia; PBB3 = pyridinyl-butadienyl-benzothiazole 3; PET = positron emission tomography; PPND = pallidopontonigral degeneration; VOIs = volumes of interest;

Introduction

Tau protein fibrillation has been implicated in Alzheimer's disease (AD), frontotemporal lobar degeneration (FTLD) subtypes and related disorders, which are collectively referred to as tauopathies.[1, 2] FTLD tauopathies, including progressive supranuclear palsy (PSP) and corticobasal degeneration (CBD), are characterized by the deposition of four-repeat tau isoforms in neurons, astrocytes, and oligodendrocytes.[3, 4] Distinct tau isoforms cause ultrastructural and conformational diversity of the pathological fibrils, represented by paired helical filaments in AD and straight filaments in PSP and CBD.[5]

Despite the association between tau conformers, localization of tau lesions, and clinical phenotypes, the symptomatic manifestations and progression of a single tauopathy can vary.[6-9] The *microtubule-associated protein tau* (*MAPT*) haplotypes may account for the clinicopathological characteristics of PSP[10] and frontotemporal dementia (FTD).[6, 11] Moreover, a number of *MAPT* mutations cause familial tauopathies, which are termed frontotemporal dementia and parkinsonism linked to chromosome 17 *MAPT* (FTDP-17-*MAPT*). However, the symptomatic profiles of patients carrying identical *MAPT* mutations are also variable.[12-16]

Evaluation of the correlation between the clinical course and chronological sequence

of regional pathological involvement has been enabled by in vivo positron emission tomography (PET) of tau lesions in humans. The radioligand [^{11}C]pyridinyl-butadienyl-benzothiazole 3 ([^{11}C]PBB3) binds to a wide range of tau fibrils including AD, PSP, and putative CBD tau deposits,[17-19] Other tracers, such as [^{18}F]AV-1451, ~~are selective~~produce a higher contrast for AD-type tau tangles ~~versus~~than it does for four-repeat tau inclusions in PSP and CBD~~.~~,[20, 21] although [^{18}F]AV-1451 has enabled differentiation between groups of PSP patients and healthy controls.[22] The distinct selectivity of the PET ligands could help identify tau isoforms contributing to unique neurodegenerative pathologies in each individual.[~~22~~22~~23~~]

The *MAPT* N279K mutation was originally discovered in the Caucasian pallidopontonegral degeneration (PPND) kindred,[~~23~~24] and was also found in three Japanese kindreds,[~~23-25~~24-26] two of which bore identical mutant *MAPT* allele haplotypes.[~~25~~27] More recently, our group reported that patients with FTDP-17-*MAPT* in three additional Japanese families with this mutation presented Parkinsonism-dominant clinical phenotypes, similar to the PPND pedigree.[~~26~~27]

In the present work, we further identified two novel Japanese families with hereditary tauopathy caused by the N279K mutation, and we investigated the abundance and extent of tau deposits in patients harboring the *MAPT* N279K mutation derived from three pedigrees including these two families. As our previous *in vitro* assays demonstrated binding of [^{11}C]PBB3 to N279K mutant four-repeat tau aggregates,[~~22~~22~~23~~] [^{11}C]PBB3-PET allowed us to analyze fibrillary tau pathologies in living patients in these families. The haplotypes of all mutant *MAPT* allele-carriers examined here were identical, presumably originating from a single founder. However, there was a profound difference in the progression of functional impairments among these three kindreds, in close association with the severity of PET-detectable tau pathologies.

Methods

Participants and genetic analysis

The current study was approved by the local ethics committees of the Juntendo University School of Medicine and National Institute of Radiological Sciences (NIRS), of which the registration numbers of University hospital medical information network (UMIN) in Japan are #000009863 and #000017978. All participants or caregivers were fully informed and provided written consent. We enrolled patients with suspected FTDP-17 who fulfilled the consensus clinical diagnostic criteria of FTLD[9] and were suspected of having a strong family history of FTD. Four of these participants were derived from a pedigree with the N279K *MAPT* mutation, which was reported previously.[26,27] We obtained the medical records and neurological findings of the patients, who were examined by at least two neurologists. We also interviewed their family members. DNA analysis was performed as described in the supplementary material and methods.

The N279K *MAPT* mutation was detected in six patients derived from two newly identified kindreds (families A and B), consisting of four males from family A and one male and one female from family B (Table 1 and Figure 1A). The third kindred with the N279K mutation (designated family C in the present study) corresponded to 'family D' in our earlier study.[26,27] Two previously reported cases of females undergoing autopsy and two new-onset females from this family were analyzed in the present study. All these members of families A, B, and C were born in the same region north of Tokyo. Kaplan-Meier survival estimation and log-rank test were performed using GraphPad Prism®6 (GraphPad Software, Inc., San Diego, CA, USA) to compare the duration of survival after disease onset among these three families.

Tau and amyloid PET imaging

PET scans were performed on four patients with the N279K *MAPT* mutation (A-II-1, B-II-2, C-IV-1 and C-IV-2) at NIRS. Two patients received scans within one year of clinical onset of the disease (at five and twelve months in C-IV-1 and B-II-2), while the other two patients underwent scans relatively late (at three and four years after onset in A-II-1 and C-IV-2, respectively). We also included 13 age- and sex-matched volunteers, who were cognitively intact, as healthy controls (HCs) in the present analysis. They were recruited from the volunteer association at NIRS, and did not have a history of neurological and psychiatric disorders or abnormalities in physical and neurological examinations. PET imaging of tau and amyloid-β lesions with [^{11}C]PBB3 and [^{11}C]Pittsburgh Compound-B ([^{11}C]PiB), respectively, were conducted for these control participants in our previous work.[13] The [^{11}C]PiB-PET data indicated that they were all negative for Aβ deposits.

Radiosynthesis of [^{11}C]PBB3 and [^{11}C]PiB was conducted as described elsewhere.[27, 28, 29] Patients underwent dynamic three-dimensional PET scans, at 50 and 70 min after intravenous injections of [^{11}C]PBB3 (injected dose, 454 ± 79 MBq; molar activity at injection, 104 ± 77 GBq/μmol; chemical purity, 97.1 ± 0.6%) and [^{11}C]PiB (injected dose, 415 ± 75 MBq; molar activity, 70 ± 7 GBq/μmol; chemical purity, 98.8 ± 0.7%), to evaluate tau and Aβ accumulations, respectively. PET data were acquired using a Siemens ECAT EXACT HR+ scanner (CTI PET Systems, Inc., Knoxville, TN), with an axial field of view of 155 mm, providing 63 contiguous 2.46-mm slices with 5.6-mm transaxial and 5.4-mm axial resolutions. Images were then reconstructed using the filtered back-projection ~~method~~algorithm (Hanning filter; cut-off frequency, 0.4 cycle/pixel~~).~~) to secure methodological consistency with our previous clinical PET works with [^{11}C]PBB3.[17, 18] Attenuation and scatter corrections were applied to these images using the data of a 10-min transmission scan, with a 68Ge-68Ga line source and single-scatter simulation method,

respectively. Three-dimensional T1-weighted magnetic resonance images (repetition time range/echo time range, 7 ms/2.8 ms; field of view [frequency × phase], 260 × 244 mm; matrix dimension, 256 × 256; 170 contiguous axial slices of 1.0 mm thickness) were acquired with a 3-T MRI scanner (Signa HDx; GE Healthcare, WI, USA, or MAGNETOM Verio, Siemens Healthcare, Erlangen, Germany) on the same day as the [^{11}C]PBB3-PET scan.

All images were preprocessed using PMOD software version 3.8 (PMOD Technologies Ltd., Zürich, Switzerland) and Statistical Parametric Mapping software (SPM12, Wellcome Department of Cognitive Neurology, London, UK), operating in the MATLAB software environment (version 9.2; MathWorks, Natick, MA, USA). Data preprocessing and data analysis of the PET images were performed as previously described.[18] Briefly, each PET image was co-registered to individual T1-weighted magnetic resonance images after motion correction, and anatomically normalized into Montreal Neurological Institute standard space (MNI152; Montreal Neurological Institute, Montreal, QC, Canada) using Diffeomorphic Anatomical Registration Through Exponentiated Lie Algebra (DARTEL).[29] We generated parametric images of the standardized uptake value ratio (SUVR) for [^{11}C]PBB3 and [^{11}C]PiB at 30–50 and 50–70 min, respectively, after radioligand injection, using the cerebellar cortex as a reference region. To estimate local tau and Aβ burdens, template volumes of interest (VOIs) were defined in several neocortical and subcortical regions, including gray and white matter of the frontal, parietal, occipital, medial and lateral temporal lobes, and the hippocampus, amygdala, caudate, putamen, globus pallidus, thalamus, anterior and posterior cingulate, substantia nigra (SN), and whole midbrain, using the automated anatomical labeling atlas implemented in PMOD software. They were modified to be devoid of CSF space using CSF maps generated from individual MRI data. Whole gray matter and whole white matter masks were also generated

from individual MRI data. In addition to VOI-based quantifications of SUVRs, we performed a voxel-by-voxel jack-knife examination of parametric SUVR images using SPM12 to statistically assess distributions of areas with an increased [^{11}C]PBB3 retention in each patient compared with 13 HCs.

Neuropathological analysis

The brains of two patients in family C (C-III-3 and C-III-4) were neuropathologically analyzed to examine if the distributions of tau pathologies in these cases agreed with those of other N279K mutant pedigrees, as previously reported.[23, 24, 30, 25, 31, 32] Clinical manifestations of these two patients were reported in our previous work, where C-III-3 and C-III-4 were designated as subjects 6 and 7 from family D, respectively.[26, 27] The pathological analysis methods were described in detail in the supplementary material and methods.

Results

Clinical and genetic analyses

An analysis of *MAPT* haplotypes revealed that all seven patients from families A, B, and C, who were examined here, shared a common single founder (Figure 1A and B). The demography and clinical profiles of all ten patients are summarized in Table 1; detailed clinical information of all patients and family members is described in the supplementary case presentation. Most of the patients manifested motor symptoms as rigid-akinesia parkinsonism at an early clinical stage, followed by exacerbated motor symptoms and cognitive decline within a few years of onset. The efficacy of levodopa treatments was limited. All patients examined were diagnosed with behavioral variant FTD, based on the

clinical diagnosis criteria of FTD.[~~32~~33] Average age at onset was 42.2 ± 5.0 years. Cognitive symptoms were initially characterized by socially inappropriate behavior, apathy, diminished social interest, and deficits in executive tasks. Apraxia of eyelids and restricted eye movements were less frequent symptoms (42.9%, 4/7). Average age at death was 48.7 ± 6.5 years. Overall disease duration from disease onset to death was very short, averaging 3.6 ± 5.4 years. Despite the haplotypic homogeneity of the mutant *MAPT* allele among the patients, Kaplan-Meier analysis depicted significant differences in the survival proportions between combined A and B families, and family C (p = 0.01 by log-rank test) (Figure 1C). Members of family C had better prognosis than those of families A and B.

PET imaging

Compared with HCs, all scanned patients had larger [^{11}C]PBB3 SUVRs in characteristic brain regions, including neocortical gray and white matter (Table 2 and Figure 2). This was distinct from the gray matter-dominant topology of tau depositions in the AD spectrum,[17, 18] and corresponded to previous [^{11}C]PBB3 autoradiographic findings.[~~22~~23] Subject C-IV-1 had the shortest interval between onset and PET scans, and exhibited a remarkable increase of [^{11}C]PBB3 SUVRs in the midbrain, including the SN, hippocampus and amygdala, suggesting that tau pathologies could arise from these regions (Figure 2). Tau deposits appeared to expand from the brainstem and limbic areas to the neocortex and subcortical nuclei with disease progression, since subject C-IV-2, who underwent PET assays 4 years after onset, presented more widespread and ~~heavier tau burdens involving~~greater increase of [^{11}C]PBB3 bindinginvolving neocortical white matter, globus pallidus and thalamus than subject C-IV-1 (Table 2).

In line with the notable difference in the rate of progression to death between families A/B and C, a subject from family B (B-II-2), who was scanned 12 months after onset, had

even higher levels of [^{11}C]PBB3~~-detectable tau accumulations~~ retentions in most ~~volumes of interest (~~VOIs~~)~~ than subject C-IV-2, despite the relatively early stage of the clinical course (Figure 2). ~~Tau deposition~~Radioligand binding in subject A-II-1, a member of family A undergoing PET examinations 3 years after onset, was comparable with that of subject B-II-2 in the majority of VOIs, although additional increases of [^{11}C]PBB3 SUVRs were noted in several areas, including the parahippocampal gyrus and amygdala (Table 2). Therefore, PET-visible tau pathologies in families A and B seemingly plateaued early during clinical progression. None of the patients were Aβ-positive according to visual and quantitative assessments of [^{11}C]PiB-PET data, which were conducted as in previous studies.[13]

In order to highlight areas with increased [^{11}C]PBB3 retentions on brain maps, we also conducted voxel-based statistical assessments of SUVR images for this tracer. SPM t-maps depicted enhanced [^{11}C]PBB3 radiosignals rather confined to the brainstem and a few other regions including the hippocampus in family C, which was in sharp contrast with increases of radioligand binding in extensive areas containing neocortical gray and white matter in families A and B (Figure 3). This familial difference was observed in subjects with both short and long durations, notwithstanding that areas highlighted in the SPM maps were somewhat increased in a manner dependent on the disease duration.

Neuropathological examinations

We obtained brain tissue from two autopsy cases, subjects C-III-3 and C-III-4, who were members of family C and died 12 and 8 years after disease onset, respectively. The brains of subjects C-III-3 and C-III-4 weighed 930 and 1030 g, respectively (Supplementary Figure ~~3A~~1A, B). Macroscopically, severe atrophic changes were observed in the pallidum and brainstem, while neocortical atrophy was moderate. Furthermore, the SN and locus

coeruleus (LC) were depigmented.

Immunohistochemical assays revealed abundant tau lesions, such as neurofibrillary tangles, pretangles, threads, coiled bodies, and tufted astrocytes, in the frontotemporal region, globus pallidus and midbrain, and to a lower extent in other neocortical and limbic areas and subcortical nuclei. Notably, tau pathology in neocortical white matter primarily consisted of axonal threads, coiled bodies and tufted astrocytes, which were more prominent than those in gray matter (Supplementary Figure ~~3F~~1F, G and Supplementary Table 1). Tau deposits were accompanied by neuronal loss and gliosis, particularly in the basal ganglia and brainstem, including the SN and LC (Supplementary Figure ~~3C~~1C-E and Supplementary Table 1). These alterations were consistent with previously documented neuropathological features of FTDP-17-*MAPT* in Caucasean[~~30,~~ 31, 32] and Japanese[~~23,~~ 24, 25] ~~patients with the N279K mutation. Further, the topology of these results corroborated with observations in tau PET imaging, except for the high [^{11}C]PBB3 retention versus relatively mild AT8(+) tau accumulation in the occipital cortex (Table 2).~~ patients with the N279K mutation. Moreover, there was high concordance between pathological characteristics of the two cases, and neurodegenerative pathologies were not overtly related to alpha-synuclein, Aβ, and TDP-43 in the patients' brains.

Discussion

We documented three Japanese families with the N279K FTDP-17-*MAPT* mutation originating from a single founder according to a haplotype analysis. Two of these kindreds (A and B) are newly identified and are characterized by markedly rapid clinical progression, leading to death within 5 years of disease onset. The third kindred (family C) examined here included two previously reported[~~26~~27] and two novel patients. The rates of clinical advancement were comparable with those of other affected members of this family[~~26~~27] and

carriers of this mutation in different Japanese[~~23-25~~24-26] and Caucasian pedigrees,[~~30,~~ 31, ~~33~~32, 34, 35] with an approximate post-onset survival period of 10 years. Hence, the present data illustrated a pronounced inter-familial difference in the aggressiveness of the illness, despite the similarity of their mutant *MAPT* allele.

Previous studies reported that patients with FTDP-17-*MAPT*, which could be linked to the same single mutation, demonstrated inter- and intra-familial heterogeneity in clinicopathological features.[12, 13, 16, ~~35~~36] FTD due to the *MAPT* intron 10 + 16 mutation presented considerable variation in age at onset and duration of the disease, both between and within families.[12] Furthermore, age at death, disease duration, clinical symptoms, brain atrophy and pathological findings, including tau deposits, were diverse, even among relatives with FTDP-17-*MAPT* caused by the P301L mutation.[16] Taken together with the present results, these observations support the view that the *MAPT* mutation alone may not fully define the clinical and neuropathological outcomes, which could in fact be modulated by other genetic and/or environmental components.

The PET results of the present study provide the first demonstration of heterogeneous neuroimaging phenotypes among patients with FTDP-17-*MAPT* who possess the same pathogenic mutation and *MAPT* allele haplotype. In close association with clinical progress, affected cases in families A and B exhibited extensive ~~accumulations~~increases of ~~tau aggregates~~[^{11}C]PBB3 binding in neocortical and subcortical areas from an early period after onset. ~~Deposition~~Enhancement of [^{11}C]PBB3~~-positive tau aggregates~~ binding, however, was less prominent in patients from family C, who had a longer clinical duration than those from the other two families. These findings indicated that the formation of tau lesions in families A and B ~~occured~~occurred rapidly at the peri-onset stage, and then almost plateaued at an early post-onset stage. This was then followed by a prompt evolution of functional deteriorations, resulting in a short lifespan of the affected members after onset. This may

also suggest the significance of tau PET as a predictor of the following neurodegenerative processes, resembling findings in patients with AD, who show a tight correlation between baseline retention of a tau PET probe and subsequent longitudinal atrophy of the cortex.[~~36~~37] Such a notion will be further examined in additional cases with the N279K mutation, and will be expandable to other diverse tauopathies by obtaining time-course evidence from a larger sample size.

The symptomatic profiles of the current N279K mutant cohort were all PSP-like, consistent with the fact that this mutation is commonly related to a Parkinsonism-predominant phenotypic presentation rather than other tau mutations.[~~33~~34] However, the manifestations of the two patients from family A were initiated with personality changes (Table 1), raising the possibility of the existence of a variable chronology of neuropsychiatric phenotypes within pedigrees of a common origin. Similar diversities were also noted in members of PPND and Italian families with the N279K mutation,[~~34~~35] and were conceived to stem from the H1/H2 haplotypes of *MAPT*.[~~37~~38] Since the Japanese population does not possess the H2 haplotype,[~~38,~~ 39, 40] the personality-related presentation of initial symptoms observed in family A, but not in the other two families, could be attributed to additional genotypic variations located on the non-mutant *MAPT* allele and/or non-*MAPT* elements.

Parkinsonian symptoms in affected individuals from family C from an early clinical stage are typical of the N279K mutation,[~~33~~34] and could be induced by involvement of the extrapyramidal tract in tau pathologies. Indeed, a profound ~~accumulation~~increase of [^{11}C]PBB3~~-capturable tau lesions~~ binding in subject C-IV-1 with a short post-onset duration was particularly evident in the SN (Table 2), which might be an initiation site of tau fibrillogenesis at a preclinical stage. This may be in line with our previous PET findings, where the nigrostriatal dopaminergic system was disrupted in presymptomatic carriers of

the N279K mutation derived from the PPND pedigree.[~~38~~39] Meanwhile, the origin of tau depositions in members of family A with initial manifestations dominated by psychiatric signs has yet to be clarified. The tau PET data of subject C-IV-1 (in the current study) also suggest that tau pathologies in the amygdala and hippocampal formation emerge early during the clinical course. This might elicit local neuronal death and atrophic changes, as illustrated by an MRI analysis of the above-mentioned N279K mutant carriers at a prodromal disease stage.[~~38~~39] Although no cognitive impairments were noted in subject C-IV-1, subclinical declines of memory functions related to hippocampal pathologies may occur, and they would be detected by specific neuropsychological test batteries.

Similar to the advancement of Braak stages of tau pathologies in the AD spectrum~~;~~[~~39~~, 40], the ~~spread~~extent of tau pathologies may reflect the disease progression in N279K mutant cases. However, the tau ~~dissemination~~pathogenesis, even in family C, appeared to be rapidly progressive relative to AD. Moreover, ~~tau lesions~~regions and voxels with increased [^{11}C]PBB3 binding in ~~cortical~~neocortical white matter ~~in~~of mutation carriers from all three families expanded over time, which differed from the gray matter-predominant distribution of tau fibrils in AD. Deposition of tau assemblies in white matter may be a neuropathological characteristic of familial[~~30~~, 31, ~~40~~32, 41, 42] and sporadic[~~42~~, 43, 44] FTLDs with an excess of insoluble four-repeat tau isoforms. In mouse models, propagation of four-repeat tau pathologies was provoked by intracranial inoculation of four-repeat tau fibrils,[45] and tau aggregates extracted from the PSP and CBD brains have been found to induce dissemination of tau fibrillogenesis in astrocytes and oligodendrocytes unlike AD brain extracts.[46] Further, the N279K mutant tau may show high propensity to intra-axonal and intercellular propagations to neighboring neurons and glial cells, in light of previous cell-based and neuropathological assays.[~~44~~47] This property of N279K mutant four-repeat tau isoforms could explain the heavy tau load in white matter

and relatively rapid regional expansion of tau accumulations in affected cases. In addition, there should be an additional molecular modifier of tau dissemination, underlying the heterogeneities of tau extent in PET imaging and phenotypic aggressiveness among the three families. Despite these presumptions, there has been no in vivo evidence for cell-to-cell propagations of tau depositions via neural networks in *MAPT* N279K mutant cases, and supportive demonstrations would need to be acquired by longitudinal PET scans of these individuals for tracking temporal changes in the topology of tau depositions.

In family C, the localization of fibrillary tau inclusions in the brains of two autopsied patients corresponded to the spatial extent of ~~PET-detectable~~ tau deposits in ~~living patients.~~previous reports on N279K mutant cases.[24, 25, 31, 32] On the basis of a neuropathological assay of local tau accumulation seemingly aligned with onsite neuronal loss, the neurotoxicity of overflowing tau species was indicated. Although more intense PET signals in multiple brain areas were observed in patients from families A and B, the regional involvement in these cases was still in general agreement with postmortem findings of the two members of family C and previous neuropathological observations in N279K mutant cases.[45~~48~~] Therefore, rather than being topological variations, the tau pathologies in families A and B are likely to follow a common trajectory of the tau pathogenesis triggered by the N279K mutation, notwithstanding the rapidness of tau expansions in these kindreds.

A few technical issues need to be considered in the interpretation of the current PET data. ~~The~~A few brain areas, such as the occipital cortex, had high [^{11}C]PBB3 retention *in vivo* despite relatively mild AT8(+) tau accumulations in neuropathological assays (Table 2). This discrepancy could arise from ~~the fact that patients with the N279K mutation exhibited remarkable radioactivity uptake in the superior sagittal sinus, and particularly in the proximity of the occipital cortex (Figure 2). Although each template VOI was modified to~~

~~be devoid of non-brain segments using CSF maps generated from individual MRI data, the spillover of radioactivity from the superior sagittal sinus might lead to overestimation of SUVR values in the occipital VOI.~~ spillover of radioactivity from the superior sagittal sinus leading to overestimation of SUVR values in the occipital VOI. However, no conclusive view on this issue could be constructed at present, as PET and postmortem data were collected from different members of family C, and an analysis of correlations between in vivo imaging and neuropathological assays in the same individuals with N279K and other MAPT mutations will be required for precise evaluations of the binding specificity of [^{11}C]PBB3 for tau pathologies in FTDP-17. Moreover, in vivo off-target binding and non-specific retention of [^{11}C]PBB3 remain undetermined. Our recent in vitro binding assays using human brain homogenates has indicated that [^{11}C]PBB3 does not cross-react with monoamine oxidases A and B,[49] which is in clear distinction from properties of other tau radioligands, including [^{18}F]AV-1451[50] and [^{18}F]THK5351.[51] This observation, however, does not fully ensure the selectivity of [^{11}C]PBB3 for tau fibrils in PET imaging of living patients with tauopathies.

In conclusion, the current study delineated the neuropathological basis of the clinical phenotypes in living patients with FTDP-17-*MAPT*, underscoring the contribution of factors beyond the disease-causative *MAPT* haplotypes and mutations to prompt the spread of tau and clinical progress. Although these modifiers are still unidentified, there could be common accelerators or decelerators of tau pathologies across a wide range of tauopathies. An expansion of the present approach combining tau PET and genetics to a large FTDP-17-*MAPT* pedigree originating from a single founder would facilitate the revelation of such elements. Moreover, our imaging assay has supported the significance of the baseline extent of tau lesions at an early clinical stage as a predictor of rapid and slow subsequent disease progressions. In the event that future clinical assays demonstrate that

this can be translated to other four-repeat tauopathies, tau PET would help to stratify an observational or interventional cohort of participants, based on an expected rate of clinical and pathological advancements.

References

1. Ballatore C, Lee VM, Trojanowski JQ. Tau-mediated neurodegeneration in Alzheimer's disease and related disorders. Nat Rev Neurosci 2007;8(9):663-672.

2. Spillantini MG, Goedert M. Tau pathology and neurodegeneration. Lancet Neurol 2013;12(6):609-622.

3. Katsuse O, Iseki E, Arai T, et al. 4-repeat tauopathy sharing pathological and biochemical features of corticobasal degeneration and progressive supranuclear palsy. Acta Neuropathol 2003;106(3):251-260.

4. Murray ME, Kouri N, Lin WL, Jack CR, Jr., Dickson DW, Vemuri P. Clinicopathologic assessment and imaging of tauopathies in neurodegenerative dementias. Alzheimers Res Ther 2014;6(1):1.

5. Quadros A, Ophelia I, Ghania A. Role of tau in Alzheimer's dementia and other neurodegenerative diseases. J Appl Biomed 2007;5:1-12.

6. Morris HR, Gibb G, Katzenschlager R, et al. Pathological, clinical and genetic heterogeneity in progressive supranuclear palsy. Brain 2002;125(Pt 5):969-975.

7. Wakabayashi K, Takahashi H. Pathological heterogeneity in progressive supranuclear palsy and corticobasal degeneration. Neuropathology 2004;24(1):79-86.

8. Lam B, Masellis M, Freedman M, Stuss DT, Black SE. Clinical, imaging, and pathological heterogeneity of the Alzheimer's disease syndrome. Alzheimers Res Ther 2013;5(1):1.

9. Respondek G, Stamelou M, Kurz C, et al. The phenotypic spectrum of progressive supranuclear palsy: a retrospective multicenter study of 100 definite cases. Mov Disord 2014;29(14):1758-1766.

10. Conrad C, Andreadis A, Trojanowski JQ, et al. Genetic evidence for the involvement of tau in progressive supranuclear palsy. Ann Neurol 1997;41(2):277-281.

11. Laws SM, Perneczky R, Drzezga A, et al. Association of the tau haplotype H2 with age at onset and functional alterations of glucose utilization in frontotemporal dementia. Am J Psychiatry 2007;164(10):1577-1584.

12. Janssen JC, Warrington EK, Morris HR, et al. Clinical features of frontotemporal dementia due to the intronic tau 10(+16) mutation. Neurology 2002;58(8):1161-1168.

13. Boeve BF, Tremont-Lukats IW, Waclawik AJ, et al. Longitudinal characterization of two siblings with frontotemporal dementia and parkinsonism linked to chromosome 17 associated with the S305N tau mutation. Brain 2005;128(Pt 4):752-772.

14. Doran M, du Plessis DG, Ghadiali EJ, Mann DM, Pickering-Brown S, Larner AJ. Familial early-onset dementia with tau intron 10 + 16 mutation with clinical features similar to those of Alzheimer disease. Arch Neurol 2007;64(10):1535-1539.

15. Larner AJ. Intrafamilial clinical phenotypic heterogeneity with MAPT gene splice site IVS10+16C>T mutation. J Neurol Sci 2009;287(1-2):253-256.

16. Tacik P, Sanchez-Contreras M, DeTure M, et al. Clinicopathologic heterogeneity in frontotemporal dementia and parkinsonism linked to chromosome 17 (FTDP-17) due to microtubule-associated protein tau (MAPT) p.P301L mutation, including a patient with globular glial tauopathy. Neuropathol Appl Neurobiol 2017;43(3):200-214.

17. Maruyama M, Shimada H, Suhara T, et al. Imaging of tau pathology in a tauopathy mouse model and in Alzheimer patients compared to normal controls. Neuron 2013;79(6):1094-1108.

18. Shimada H, Kitamura S, Shinotoh H, et al. Association between Abeta and tau accumulations and their influence on clinical features in aging and Alzheimer's disease spectrum brains: A [11C]PBB3-PET study. Alzheimers Dement (Amst) 2017;6:11-20.

19. Perez-Soriano A, Arena JE, Dinelle K, et al. PBB3 imaging in Parkinsonian disorders: Evidence for binding to tau and other proteins. Mov Disord 2017;32(7):1016-1024.

20. Marquie M, Normandin MD, Vanderburg CR, et al. Validating novel tau positron emission tomography tracer [F-18]-AV-1451 (T807) on postmortem brain tissue. Ann Neurol 2015;78(5):787-800.

21. Marquie M, Normandin MD, Meltzer AC, et al. Pathological correlations of [F-18]-AV-1451 imaging in non-alzheimer tauopathies. Ann Neurol 2017;81(1):117-128.

~~22~~22. Schonhaut DR, McMillan CT, Spina S, et al. ^{18}F-flortaucipir tau positron emission tomography distinguishes established progressive supranuclear palsy from controls and Parkinson disease: A multicenter study. Ann Neurol 2017;82:622-634.

23. Ono M, Sahara N, Kumata K, et al. Distinct binding of PET ligands PBB3 and AV-1451 to tau fibril strains in neurodegenerative tauopathies. Brain 2017;140(3):764-780.

~~23~~24. Yasuda M, Kawamata T, Komure O, et al. A mutation in the microtubule-associated protein tau in pallido-nigro-luysian degeneration. Neurology 1999;53(4):864-868.

~~24~~25. Arima K, Kowalska A, Hasegawa M, et al. Two brothers with frontotemporal dementia and parkinsonism with an N279K mutation of the tau gene. Neurology 2000;54(9):1787-1795.

~~25~~26. Tsuboi Y, Baker M, Hutton ML, et al. Clinical and genetic studies of families with the tau N279K mutation (FTDP-17). Neurology 2002;59(11):1791-1793.

~~26~~27. Ogaki K, Li Y, Takanashi M, et al. Analyses of the MAPT, PGRN, and C9orf72 mutations in Japanese patients with FTLD, PSP, and CBS. Parkinsonism Relat Disord 2013;19(1):15-20.

~~27~~28. Hashimoto H, Kawamura K, Igarashi N, et al. Radiosynthesis, photoisomerization, biodistribution, and metabolite analysis of 11C-PBB3 as a clinically useful PET probe for imaging of tau pathology. J Nucl Med 2014;55(9):1532-1538.

~~28~~29. Kimura Y, Ichise M, Ito H, et al. PET Quantification of Tau Pathology in Human Brain with 11C-PBB3. J Nucl Med 2015;56(9):1359-1365.

~~29~~30. Ashburner J. A fast diffeomorphic image registration algorithm. Neuroimage 2007;38(1):95-113.

~~30~~31. Wszolek ZK, Pfeiffer RF, Bhatt MH, et al. Rapidly progressive autosomal dominant parkinsonism and dementia with pallido-ponto-nigral degeneration. Ann Neurol 1992;32(3):312-320.

~~31~~32. Delisle MB, Murrell JR, Richardson R, et al. A mutation at codon 279 (N279K) in exon 10 of the Tau gene causes a tauopathy with dementia and supranuclear palsy. Acta Neuropathol 1999;98(1):62-77.

~~32~~33. Rascovsky K, Hodges JR, Knopman D, et al. Sensitivity of revised diagnostic criteria for the behavioural variant of frontotemporal dementia. Brain 2011;134(Pt 9):2456-2477.

~~33~~34. Tsuboi Y, Uitti RJ, Delisle MB, et al. Clinical features and disease haplotypes of individuals with the N279K tau gene mutation: a comparison of the pallidopontonigral degeneration kindred and a French family. Arch Neurol 2002;59(6):943-950.

~~34~~35. Soliveri P, Rossi G, Monza D, et al. A case of dementia parkinsonism resembling progressive supranuclear palsy due to mutation in the tau protein gene. Arch Neurol 2003;60(10):1454-1456.

~~35~~36. Lin HC, Lin CH, Chen PL, Cheng SJ, Chen PH. Intrafamilial phenotypic heterogeneity in a Taiwanese family with a MAPT p.R5H mutation: a case report and literature review. BMC Neurol 2017;17(1):186.

~~36~~37. La Joie R, Visani A, Bourakova V, et al. AV1451-PET CORTICAL UPTAKE AND REGIONAL DISTRIBUTION PREDICT LONGITUDINAL ATROPHY IN ALZHEIMER'S DISEASE. Alzheimer's & Dementia: The Journal of the Alzheimer's Association 2017;13(7):P769.

~~37~~38. Woodruff BK, Baba Y, Hutton ML, et al. Haplotype-phenotype correlations in kindreds with the N279K mutation in the tau gene. Arch Neurol 2004;61(8):1327; author reply 1327.

~~38~~39. Miyoshi M, Shinotoh H, Wszolek ZK, et al. In vivo detection of neuropathologic changes in presymptomatic MAPT mutation carriers: a PET and MRI study. Parkinsonism Relat Disord 2010;16(6):404-408.

~~39~~40. Braak H, Braak E. Neuropathological stageing of Alzheimer-related changes. Acta Neuropathol 1991;82(4):239-259.

~~40~~41. Sima AA, Defendini R, Keohane C, et al. The neuropathology of chromosome 17 - linked dementia. Ann Neurol 1996;39(6):734-743.

~~41~~42. Spillantini MG, Goedert M, Crowther RA, Murrell JR, Farlow MR, Ghetti B. Familial multiple system tauopathy with presenile dementia: a disease with abundant neuronal and glial tau filaments. Proc Nat Acad Sci U S A 1997;94(8):4113-4118.

~~42~~43. Forman MS, Zhukareva V, Bergeron C, et al. Signature tau neuropathology in gray and white matter of corticobasal degeneration. Am J Pathol 2002;160(6):2045-2053.

~~43~~44. Williams DR, Holton JL, Strand C, et al. Pathological tau burden and distribution distinguishes progressive supranuclear palsy-parkinsonism from Richardson's syndrome. Brain 2007;130(6):1566-1576.

~~44~~45. Clavaguera F, Bolmont T, Crowther RA, et al. Transmission and spreading of tauopathy in transgenic mouse brain. Nat Cell Biol 2009;11:909-913.

46. Narasimhan S, Guo JL, Changolkar L, et al. Pathological Tau Strains from Human Brains Recapitulate the Diversity of Tauopathies in Nontransgenic Mouse Brain. J Neurosci 2017;37:11406-11423.

47. Wren MC, Zhao J, Liu CC, et al. Frontotemporal dementia-associated N279K tau mutant disrupts subcellular vesicle trafficking and induces cellular stress in iPSC-derived neural stem cells. Mol Neurodegener 2015;10:46.

~~45~~48. Slowinski J, Dominik J, Uitti RJ, Ahmed Z, Dickson DD, Wszolek ZK. Frontotemporal dementia and Parkinsonism linked to chromosome 17 with the N279K tau mutation. Neuropathology 2007;27(1):73-80.

49. Ni R, Ji B, Ono M, et al. Comparative In Vitro and In Vivo Quantifications of Pathologic Tau Deposits and Their Association with Neurodegeneration in Tauopathy Mouse Models. J Nucl Med 2018;59:960-966.

50. Vermeiren C, Motte P, Viot D, et al. The tau positron-emission tomography tracer AV-1451 binds with similar affinities to tau fibrils and monoamine oxidases. Mov Disord 2018;33:273-281.

51. Ng KP, Pascoal TA, Mathotaarachchi S, et al. Monoamine oxidase B inhibitor,

selegiline, reduces ^{18}F-THK5351 uptake in the human brain. Alzheimers Res Ther 2017;9:25.

Figure legends

Figure 1. Genetic and clinical profiles of FTDP-17-*MAPT* patients derived from three families with the N279K *MAPT* mutation

(A) Pedigrees of families A, B and C. Each family originated from the same rural area with autosomal dominant inheritance, manifesting young-onset Parkinsonism and progressive cognitive decline. Filled symbols denote patients with Parkinsonism and cognitive decline, while 'm' indicates confirmed carriers of the N279K mutation. Slashed symbols denote deceased individuals; autopsied cases are indicated by asterisks. (B) Haplotype analysis of the patients showed similar gene dosage as measured by GeneMapper and identical single nucleotide polymorphisms (SNPs) in the region of *MAPT*, indicating that all these families share a common founder. (C) Kaplan-Meier survival curves for 10 patients from combined A and B families (dashed line; n = 6) and family C (solid line; n = 4). Log-rank test indicated that families A and B exhibited shorter post-onset lifespan than family C (p = 0.01).

Figure 2. [^{11}C]PBB3-PET images of representative cognitively healthy control and patients with N279K mutant FTDP-17-*MAPT*

Axial parametric SUVR images, acquired at 30–50 min after radioligand injection, were superimposed on the corresponding magnetic resonance images. All patients showed noticeable uptake of [^{11}C]PBB3 in multiple brain regions and the superior sagittal sinus (yellow arrowheads). ~~The patient with the shortest disease duration already showed remarkable uptake of [^{11}C]PBB3 in several areas, as exemplified by midbrain (white arrows) and medial temporal cortex.~~

Figure 3. ~~**Pathological findings in two affected members**~~**Localization of** ~~**family C**~~**increased [^{11}C]PBB3 retention in each patient compared with HCs**

~~(A, B) Macroscopic pictures of the brains of subjects C-III-3 (A) and C-III-4 (B). Both brains showed marked atrophic changes in the frontal lobe and brainstem. (C) Severe loss of pigmented neurons in the substantia nigra (SN; Kleihauer-Betke stain). (D, E) Hematoxylin and eosin (HE) staining also revealed profound neuronal loss and gliosis in the globus pallidus (D) and SN (E). (F) Tau-positive neuronal and glial inclusions, composed of neurofibrillary tangles, threads and coiled bodies in the globus pallidus (AT8 immunostaining). Panels B-F were derived from subject C-III-4. (G) A semi-quantitative analysis of tau aggregation in subjects C-III-3 and C-III-4. Areas with high, moderate, and low tau burdens are colored in red, yellow, and blue, respectively. These scores were determined by averaging data of the two patients.~~ Voxels with an increase of [^{11}C]PBB3 SUVR was highlighted in coronal (top), axial (middle) and sagittal (bottom) SPM t-maps. A patient with the shortest disease duration (C-IV-1) already showed remarkable enhancement of [^{11}C]PBB3 binding in several areas including the midbrain (white arrows) and medial temporal cortex (yellow arrowheads). Members of families A and B exhibited more extensive [^{11}C]PBB3 radiosignals particularly in neocortical gray and white matter than cases derived from family C.

Figure 1

(A)

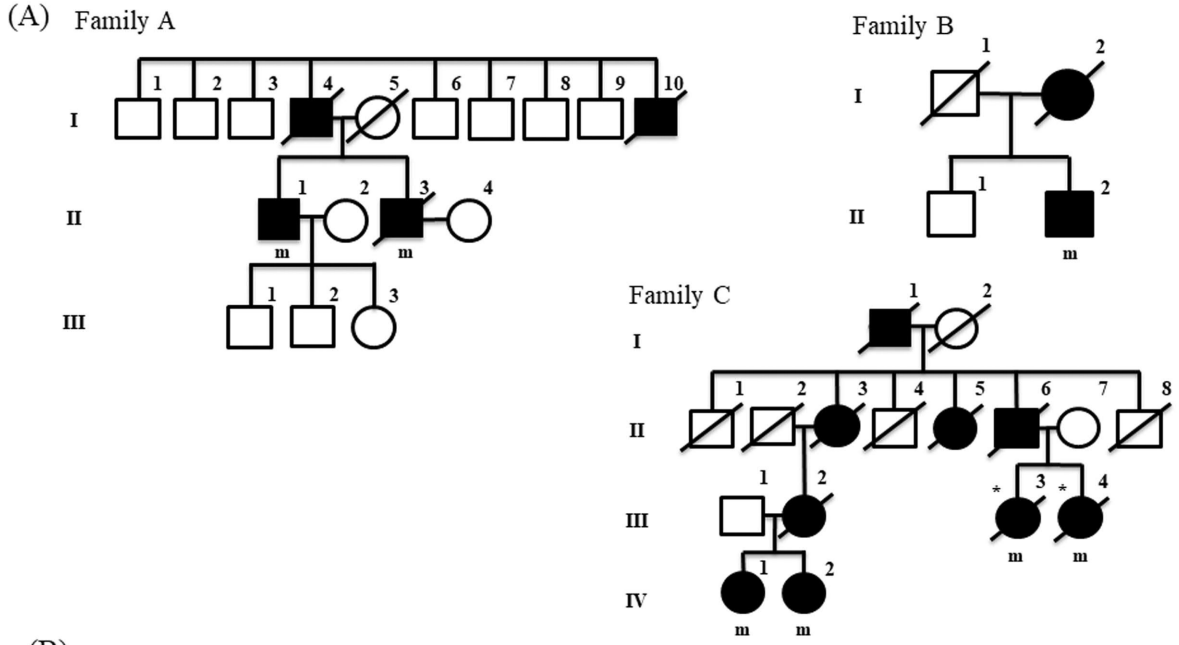

(B)

		Family A				Family B		Family C							
		A-II-1		A-II-3		B-II-2		C-III-3		C-III-4		C-IV-1		C-IV-2	
	D17S805	231	221	231	221	231	231	231	231	231	219	231	219	231	219
	D17S798	231	231	231	231	231	231	231	231	231	229	231	229	231	229
	D17S800	247	247	247	247	249	241	247	245	247	241	247	241	247	241
	D17S810	241	241	241	241	241	241	241	241	241	241	241	241	241	241
	rs1467967	A	A	A	G	A	A	A	G	A	A	A	G	A	G
	rs242557	G	G	G	G	G	G	G	A	G	A	G	A	G	A
	rs3785883	G	G	G	G	G	G	G	G	G	G	G	A	G	A
MAPT	rs2471738	T	C	T	T	T	T	T	C	T	T	T	C	T	C
	c.837T>G	G	T	G	T	G	T	G	T	G	T	G	T	G	T
	del-in9	no	no	no	no	no	no	no	no	no	no	no	no	no	no
	rs7521	G	A	G	G	G	G	G	A	G	G	G	G	G	G
	D17S806	183	151	183	151	175	175	183	187	175	173	183	155	183	155
	D17S797	172	172	172	172	172	172	172	170	172	172	172	172	172	172
	D17S809	270	268	270	276	270	278	270	278	270	270	270	276	270	276

(C)

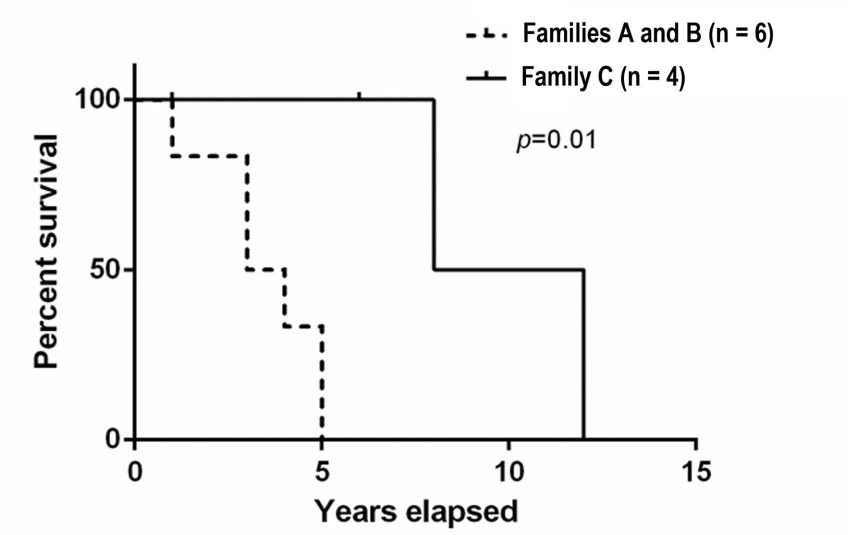

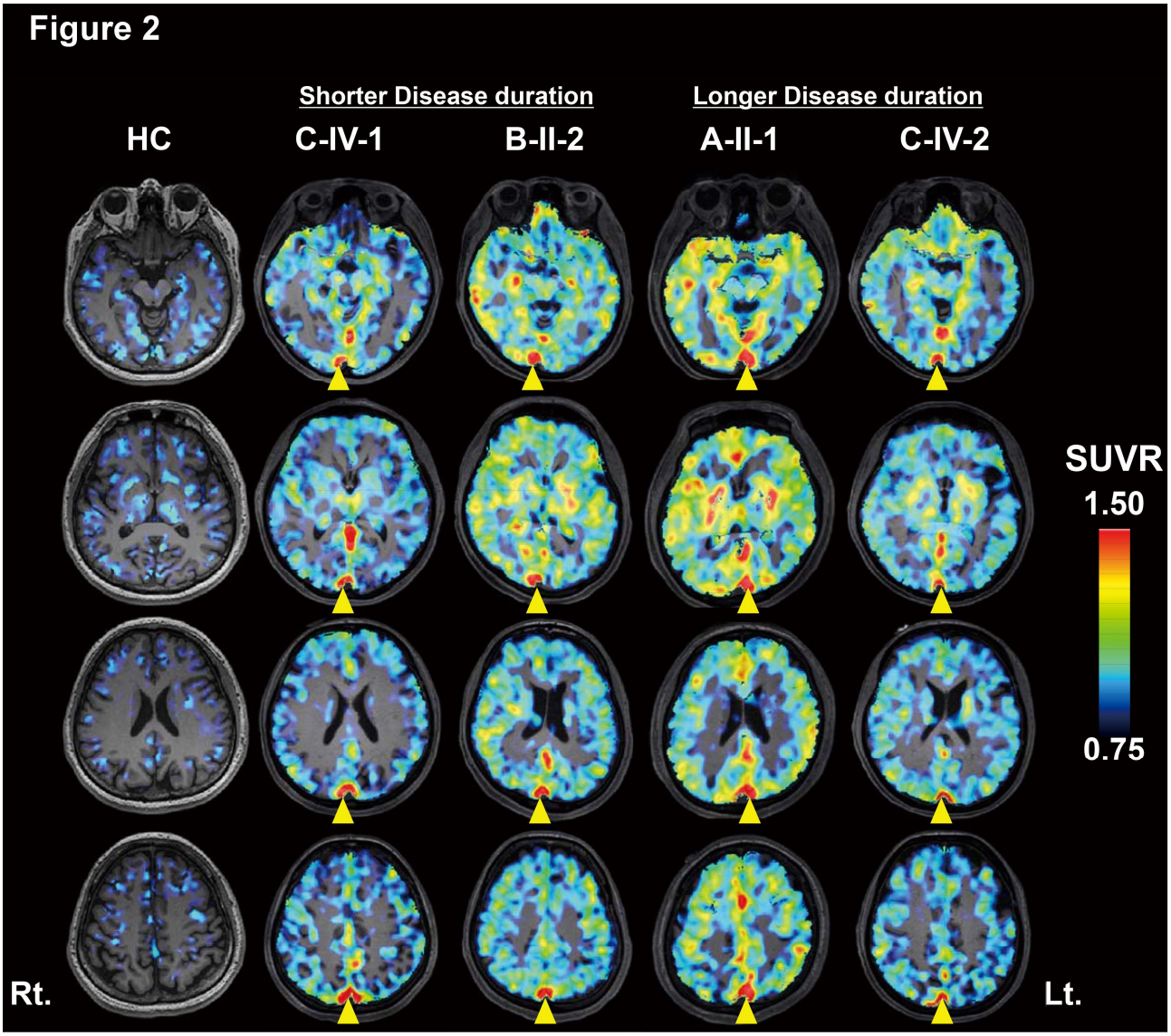
Figure 2
Shorter Disease duration
Longer Disease duration
HC
C-IV-1
B-II-2
A-II-1
C-IV-2
SUVR
1.50
0.75
Rt.
Lt.

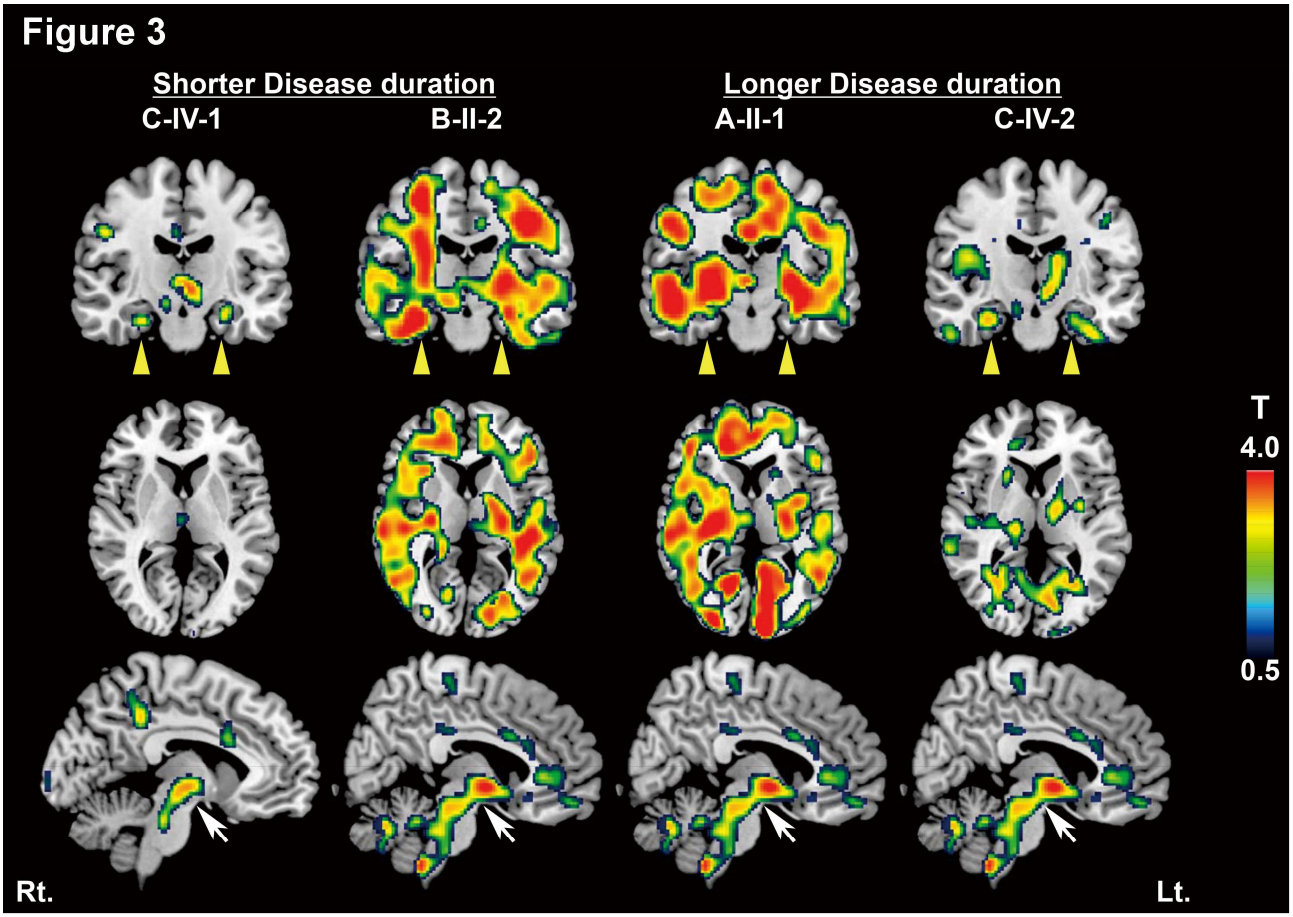
Figure 3
Shorter Disease duration
Longer Disease duration
C-IV-1
B-II-2
A-II-1
C-IV-2
T
4.0
0.5
Rt.
Lt.